Title
High Linear Energy Transfer Radiolysis of Solvent Extraction Ligands

Author
Pearson, Jeremy

Publication Date
2014

Peer reviewed|Thesis/dissertation

UNIVERSITY OF CALIFORNIA,
IRVINE

High Linear Energy Transfer Radiolysis of Solvent Extraction Ligands

DISSERTATION

submitted in partial satisfaction of the requirements
for the degree of

DOCTOR OF PHILOSOPHY

in Chemical Engineering

by

Jeremy David Pearson

Dissertation Committee:
Professor Mikael Nilsson, Chair
Professor Martha Mecartney
Professor George Miller

2014

DEDICATION

To

My Father, Mother, Wife and Family,
to little Johnny, Jayden, and Joseph

and a quote of inspiration:

"I (Leo Szilard) met him again in Berlin and there ensued a memorable conversation. Otto Mandl said that now he really thought he knew what it would take to save mankind from a series of ever-recurring wars that could destroy it. He said that Man has a heroic streak in himself. Man is not satisfied with a happy idyllic life: he has the need to fight and to encounter danger. And he concluded that what mankind must do to save itself is to launch an enterprise aimed at leaving the earth. On this task he thought the energies of mankind could be concentrated and the need for heroism could be satisfied. I remember very well my own reaction. I told him that this was somewhat new to me, and that I really didn't know whether I would agree with him. The only thing I could say was this: that if I came to the conclusion that this was what mankind needed, if I wanted to contribute something to save mankind, then I would probably go into nuclear physics, because only through the liberation of atomic energy could we obtain the means which would enable man not only to leave the earth but to leave the solar system."

Richard Rhodes
"The Making of the Atomic Bomb"
(Rhodes 1986)

TABLE OF CONTENTS

LIST OF FIGURES

LIST OF TABLES

ACKNOWLEDGMENTS

I would like to express the deepest appreciation to my committee chair, Professor Mikael Nilsson, who selected me to work on this project and expressed confidence that I could manage and perform well in the field of nuclear science, which was relatively new to me. I am grateful for his advice and friendly counsel, his bright enthusiasm for the field, direction to attend and present at many conferences even when our results were very new, and especially his encouragement to dust off and revamp decades-old gas chromatograph equipment which in the end delivered some of our best results!

I would like to thank my committee members, Professor Martha Mecartney and Professor George Miller, for their support throughout my degree; Professor Mecartney for her welcoming reception when I first arrived at UC Irvine and her enthusiasm and support throughout my degree; Professor George Miller for his enormous support and innumerable questions answered to help me get up to speed with many aspects of nuclear science and technology and topics relating to my dissertation.

I would also like to thank Jonathan Wallick, for his support with reactor runs and answering questions, and members of the Nuclear Lab and Department of Chemical Engineering and Materials Science who offered support and friendship over the past five years, making the degree a very enjoyable and memorable experience.

A very special thanks to UCI Director of Federal Relations Kathy Eiler, Dean of Engineering Gregory Washington, Vice Chancellor Wendell Brase, and Dr. Michael Prather of the Earth Systems Science Department for their support in exploring and participating in the policy side of nuclear science and technology, as well as in understanding the important aspects of climate change and the environment.

I thank Taylor and Francis (Solvent Extraction and Ion Exchange), Springer (Journal of Radioanalytical and Nuclear Chemistry), and the Royal Society of Chemistry (Journal of the Chemical Society) for permission to include copyrighted data and figures as part of my thesis/dissertation.

I thank the U.S. Department of Energy for funding and express gratitude to a society and government infrastructure which is set up to value funding for such research. This project was funded by the U.S. Department of Energy through the Nuclear Energy University Program (NEUP) project no. DE-AC07-05ID14517. I hope by my future endeavors, to prove this to be a valuable investment and give back to a society and government through the skills and opportunities that I have received as a result of this support.

CURRICULUM VITAE

Jeremy Pearson

1996-02	B.S. in Chemical Engineering, Brigham Young University
1997-99	Mission, Paraguay, The Church of Jesus Christ of Latter Day Saints
2003-05	Manufacturing Associate, Amgen Thousand Oaks, California
2006-09	Engineer, Amgen Thousand Oaks, California
2011	M.S. in Chemical Engineering, University California, Irvine
2013,14	Nuclear Engineering Student Delegation Washington D.C.
2013,14	Empowering Sustainability Fellow University of California, Irvine
2014	Ph.D. in Chemical Engineering, University of California, Irvine

FIELD OF STUDY

Solvent Extraction, Radiolysis, and Used Nuclear Fuel Recycling

PUBLICATIONS

1. J Pearson, O Jan, GE Miller, M Nilsson, *Studies of high linear energy transfer dosimetry by $^{10}B(n,\alpha)^{7}Li$ reactions in aqueous and organic solvents*, J Radioanal Nucl Chem (2012) 292:719-727
2. J Pearson, O Jan, A Wariner, GE Miller, M Nilsson, *Development of a method for high LET irradiation of liquid systems*, J Radioanal Nucl Chem (2013) 298:1401-1409
3. J Pearson, M Nilsson, *Radiolysis of tributyl phosphate by particles of high linear energy transfer*, J Solvent Extraction and Ion Exchange (2014) 32:584-600
4. BJ Mincher, SP Mezyk, G Elias, GS Groenewold, C Ekberg, G Skarnemark, JA LaVerne, M Nilsson, J Pearson, NC Schmitt, RD Tillotson, *The radiation chemistry of CMPO: Part 2. Alpha Radiolysis*, J Solvent Extraction and Ion Exchange (2014) 32(*2*):167-178

ABSTRACT OF THE DISSERTATION

High Linear Energy Transfer Radiolysis of Solvent Extraction Ligands
By

Jeremy David Pearson

Doctor of Philosophy in Chemical Engineering

University of California, Irvine, 2014

Professor Mikael Nilsson, Chair

The response to high linear energy transfer (LET) radiation of a variety of aqueous systems such as biological systems and the Fricke dosimeter has frequently been studied in the literature. Linear energy transfer is a unique property of radiation which describes the special distribution with which energy from radiation is deposited and concentrated as it travels through matter and can have implications on degradation within the matter itself. The four types of ionizing radiation alpha, beta, gamma, and neutrons have different LET, classified from low for gamma and beta, to high for alpha. All types of ionizing radiation are encountered in used nuclear fuel. This radiation induces damage to solvent extraction processes designed to recycle used nuclear fuel which results in impaired selectivity and reduced process efficiencies. While the effects of low LET radiation on organic solutions have been widely studied, the effects of high LET radiation have not due to difficulties in studying this type of radiation such as short radiation path lengths on the order of 50 μm. This study investigates the effects of high LET radiation deposited *in situ* from fission products lithium and helium emitted in the $^{10}B(n,\alpha)^{7}Li$ reaction. The reaction, studied previously in aqueous systems, is applied here to organic solvents containing ligands used

in solvent extraction. Ligands studied were TBP, CMPO, and TODGA utilized in the PUREX and TRUEX processes. Results demonstrate that high LET radiation has the tendency to reduce degradation to the parent compound due to reactive products being consumed within the radiation track, while also encouraging secondary degradation products to occur within the radiation track. Products of these secondary degradation reactions may be more detrimental to the solvent extraction process than primary degradation products and are therefore important to understand and monitor. Results also demonstrate the utility of using the $^{10}B(n,\alpha)^{7}Li$ reaction to study the effects of high LET radiation on organic solutions encountered in used nuclear fuel recycling processes. Understanding the effects of both high and low LET radiation on solvent extraction processes will facilitate early screening of novel ligand susceptibility to radiation induced degradation and also provide a more comprehensive picture of degradation encountered during radiolysis.

1. INTRODUCTION AND BACKGROUND

1.1 Nuclear Energy and Solvent Extraction

Nuclear energy is a limited resource based on a finite uranium supply. However the way in which uranium is utilized may allow nuclear energy to enter the realm of sustainability considering that uranium resources could last up to billions of years, or the remaining expected lifetime of the sun, if new extraction technologies are developed and recycling technologies are incorporated into the fuel cycle (Cohen 1983). New generation nuclear technologies which employ fast neutron spectrums in particular can benefit from reusing nuclear fuel (Stieglitz 1983). This expansion of nuclear energy and used fuel recycling technologies will occur based on their ability to compete with existing uranium prices and available technology, both fossil fuel and renewable in the future. Although the Plutonium Uranium Redox EXtraction (PUREX) (Mathur 2001) process is currently carried out industrially to recycle plutonium and uranium, the vast majority of recycling techniques, both those involving solvent extraction and pyroprocessing, are under development (Mathur 2001, Inoue 2008). Continued investigation and optimization of these recycling technologies will secure their place in future nuclear fuel cycles.

Solvent extraction processes are designed to separate reusable and waste components of used nuclear fuel which consist of the original uranium fuel, fission products such as lanthanides and precious metals, and activation products of uranium or actinides such as plutonium, americium and curium. In this process an extraction ligand is dissolved in organic diluents and contacted with nuclear fuel dissolved in an aqueous acidic solution, typically nitric acid, to extract desirable used fuel elements. The division between what is considered waste and useful in the used fuel is dynamic, as new uses can be found

for a variety of the products, and favorable economics can make production viable for elements in used nuclear fuel that are already considered to have value.

Current processes being explored in the United States for recycling used nuclear fuel are the PUREX process for recycling U and Pu, the TRansUranic Extraction (TRUEX) (Mathur 2001) process for separating the actinides and lanthanides from other fission products, and the Trivalent Actinide-Lanthanide Separation by Phosphorus reagent Extraction from Aqueous Komplexes (TALSPEAK) (Weaver 1964) process for separating the actinides from the lanthanides. There is also effort underway to consolidate the TRUEX and the TALSPEAK processes into one process called the Actinide Lanthanide Separation (ALSEP) process (Gelis 2014). The extraction ligands utilized in these processes are tributyl phosphate (TBP), n-octyl(phenyl)-N,N-diisobutylcarbamoylphosphin oxide(CMPO), and di-(2-ethylhexyl)phosphoric acid (HDEHP). N,N,N',N'-tetraoctyldiglycolamide (TODGA) is also being researched as an alternative to CMPO, as well as N,N-dimethyl-N,N-dioctyl-2,(2-hexyloxyethyl) malonamide (DMDOHEMA) used in the DIAMide EXtraction (DIAMEX) process in the European Union (Madic 2002). (Figure 1)

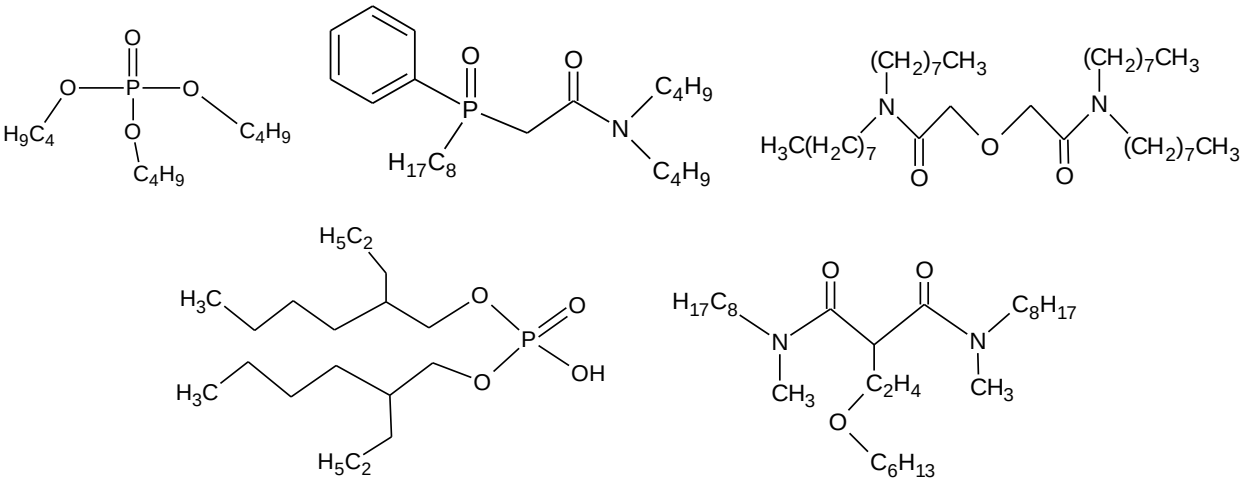

Figure 1. Extraction ligands TBP, CMPO, TODGA, HDEHP, and DMDOHEMA.

1.2 Degradation to solvent extraction processes

One of the challenges that solvent extraction processes face is degradation of the solvent and extraction ligands due to the harsh process conditions. This degradation can negatively affect the process in a variety of ways. The immediate effect is degradation/alteration of the extractant and diluent molecules. Degradation to the extractant will reduce its concentration. The properties of the degradation products are also a concern. Degradation to both the diluent and extractant can introduce new and altered extraction and solution characteristics which are nearly always undesirable (Healy 1976, Stieglitz 1983). For example, in the PUREX process TBP coextracts tetravalent and hexavalent metals U and Pu with nitric acid and works best at high nitric acid levels (Schulz 1984). Contact with a low nitric acid concentration aqueous solution can allow the Pu and U to be stripped back out into a more workable aqueous phase. TBP however degrades to dibutyl phosphoric acid which extracts best at low acid concentrations (Lloyd 1985). Under these conditions, when the organic solution is contacted with the strip phase, DBP will hold back a portion of the Pu and extract other elements such as Zr, negatively impacting separation factors. Fortunately, DBP can be washed out with a caustic wash (Stieglitz 1983), however long chain acid alkyl phosphates formed as well as hydroxamic acids resulting from nitration and oxidation of the diluent which both act similarly to DBP, are not easily removed with a caustic wash and may build up after continuous solvent recycle (Stieglitz 1983, Tripathi 1999).

These long chain acid alkyl phosphates, and diluent degradation products such as alkyl carbonic acids, nitro alkanes, and alkyl nitrates, also act as surfactants and can increase disengagement time of the organic and aqueous phases. After contacting/mixing

the two phases, the aqueous and organic phases must be physically separated using equipment such as mixer settlers. Degradation products may increase holdup time in these pieces of equipment, and can even at high concentrations create emulsions known as third phases that impede separation and disrupt normal equipment function.

In an industrial setting various analytical quality tests may be employed to monitor the extent of degradation. For example, a conductivity measurement of a sample equilibrated with sodium bicarbonate can be used to determine the content of high molecular weight acid alkyl phosphates and carboxylic acids (Stollenwerk 1989). Measuring interfacial surface tension of the same samples reflects the combined surface surfactant effect of both types of acid compounds (Stollenwerk 1989). Polarographic methods may be employed to determine the presence of nitroalkane and alkylnitrate type compounds (Stollenwerk 1989). We have chosen to focus on investigating and understanding the fundamental chemistry of what produces these products. Understanding these fundamental principles can help predict and monitor, anticipate, control, and prevent these undesirable conditions from occurring during a solvent extraction process.

There are various process conditions that contribute to these fundamental degradation processes. The most important include the presence of gases (e.g. oxygen, nitrogen), water, acid (e.g. nitric acid), radiation, metal ions, the temperature and mixing conditions, ligand concentration (i.e. ligand/diluents ratio), and type of diluent (Schulz 1984). These conditions may enhance or inhibit degradation of the parent ligand, and influence to what extent individual degradation pathways are followed and which degradation products accumulate.

Diluent type plays a key role, in particular with regards to radiation effects. Radiation will directly break down both ligand and diluents, and degradation products of diluents can be reactive enough to chemically degrade additional diluent and ligand molecules and *vice versa* (Holland 1978). TBP is more sensitive to radiation in carbon tetrachloride (CCl_4) than n-dodecane due to reactive products of CCl_4 (Burger 1958). Furthermore, it has been demonstrated that reactive products originating from the diluent, including n-dodecane, may preferentially attack ligands due to the ligand's inherent polar nature which is necessary for their extraction characteristics (Wilkinson 1961, Holland 1978). This enhances degradation of the ligand above that which would be expected if radiation damaged ligand and diluents equally according to their mass or electron fractions present (Figure 2).

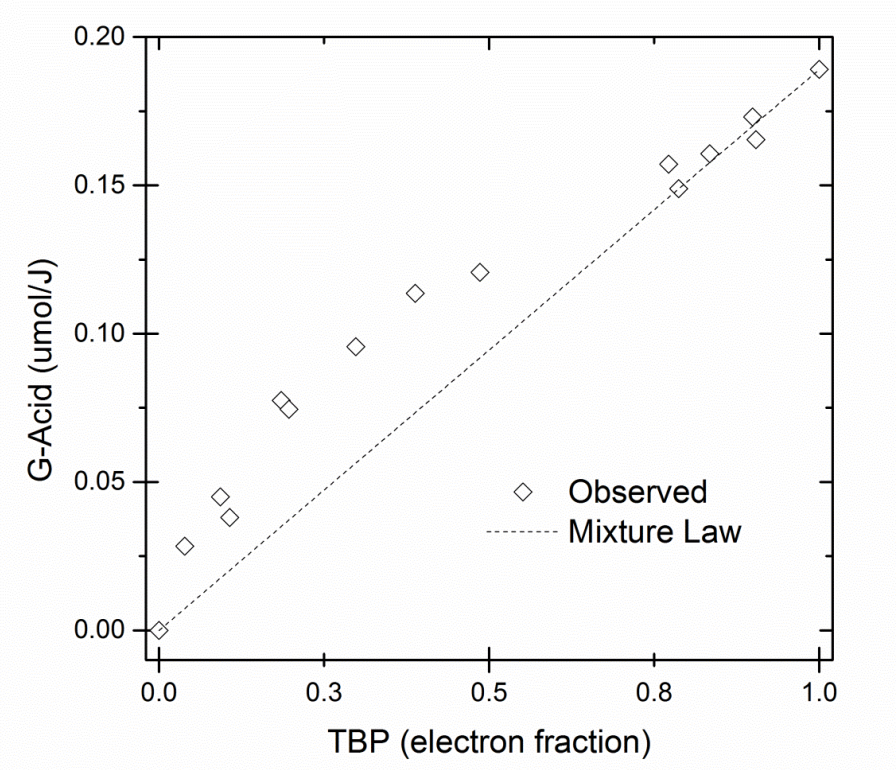

Figure 2. G-acid as a function of electron fraction of TBP in kerosene-hydrocarbon diluent, ε(TBP). (Adapted from Wilkinson and Williams (Wilkinson 1961) with permission from the Royal Chemical Society).

The presence of non-noble reactive gases and water has been shown in the case of TBP radiolysis to reduce the formation of DBP (Holland 1978, Schulz 1984). This may be due to a protective effect against direct radiolysis of TBP in the case of water which is bound to TBP (Williams 1957), or protection from indirect radiolysis by consumption of reactive products by non-noble gases such as oxygen and nitrous oxide. The presence of nitric acid stimulates acid hydrolysis of TBP to DBP and does so at increasing rates with increasing temperature (Stieglitz 1984, Lloyd 1985). Nitric acid, which also binds in solution to TBP, may have an influence on radical production from radiation (Broshkevich 1973). Nitric acid also forms the nitroalkane and alkylnitrate type compounds discussed above which can convert into hydroxamic acids. Metal ions can protect or catalyze degradation (Lloyd 1985, Mincher B. J. 2009). Combination of two TBP molecules, and TBP and diluent molecules through radical addition are often called polymer products and are the origin of high molecular weight acid alkyl phosphates described above. A summary of these reactions is shown in Figure 3 for TBP as an example. Acid compounds are typically formed through secondary reactions, with the exception of DBP in TBP radiolysis, and are generally the major culprits cited in performance loss to solvent extraction processes based on TBP (i.e. PUREX).

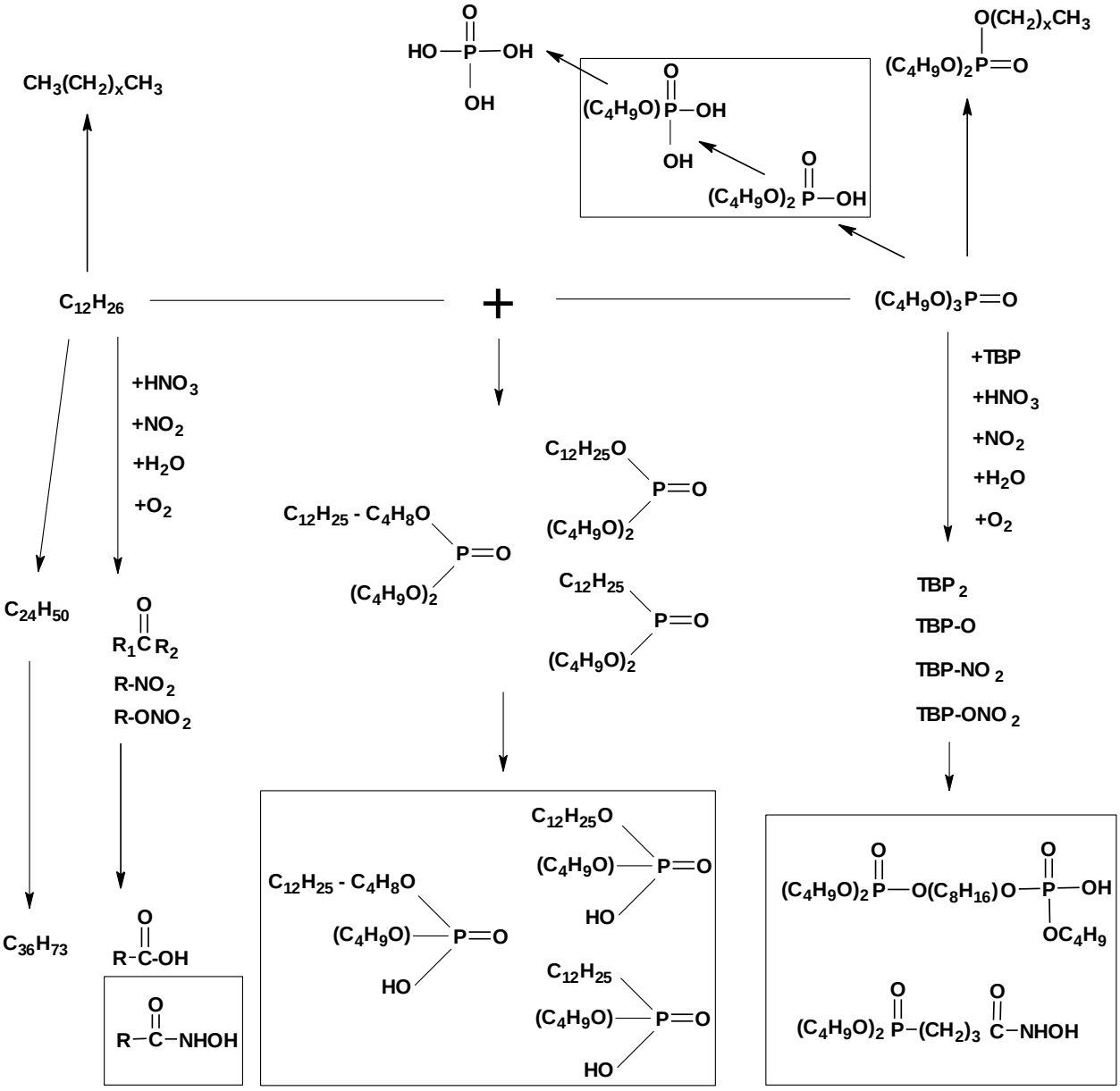

Figure 3. Degradation cascade of TBP and organic diluent. Boxed molecules represent acidic products which may have undesirable extraction characteristics. Those with high molecular weight towards the bottom of the figure are the most challenging to remove.

1.2.1 Degradation by radiolysis and radiation types

One of the factors determining the type and extent of degradation to a solvent extraction process is the type of radiation. Used nuclear fuel contains all four types, gamma, beta, alpha, and neutron radiation. Alpha radiation has been considered a major culprit in the

formation of secondary acid products (Hui-bo 2012) due to the manner in which energy is deposited for this type of radiation. Radiation can be classified by linear energy transfer (LET) which describes the rate of energy deposition per unit distance. Gamma and beta radiation are considered low (LET) radiation, depositing their energy sparsely over a large distance. This type maximizes indirect or sensitized radiolysis reactions (Wilkinson 1961, Holland 1978). On the other hand, alpha radiation is considered high LET, depositing its energy very densely over a much shorter distance. This can result in depressed degradation of parent ligands compared to gamma as observed by Sugo et al. (Sugo 2009) in their irradiations of TODGA as reactive products are consumed or rendered benign in the track. It also confines the reaction chemistry to the track with molecules that have already reacted once, increasing the formation of acidic molecules and secondary products as observed in the work of Hui-bo (Hui-bo 2012)(Figure 3). The differences in these radiation types can be visualized by cloud chamber images (Figure 4).

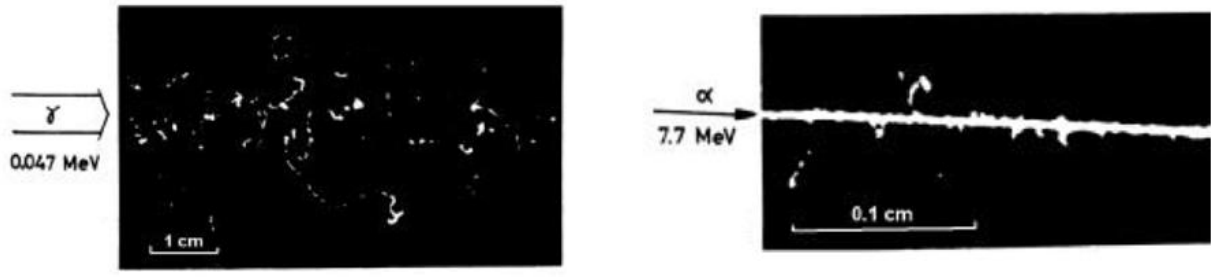

Figure 4. Gamma and alpha tracks in a cloud chamber (Genter 1954).

Studying the unique effects of both gamma and alpha radiation is therefore very important to understanding the radiation chemistry of a solvent extraction process. Individual processes will be exposed at different levels to gamma/beta (low LET) and alpha

(high LET) radiation. Lanthanides and fission products typically emit gamma/beta radiation, while many actinides emit alpha radiation in addition to gamma/beta radiation. Plutonium, americium, and curium especially, have isotopes with high alpha activity and deposit a significant amount of alpha dose. The actinides are generally the most desirable for recycling, since they can be reused for fission, so in a solvent extraction process close attention to whether they are extracted into the organic/ligand phase where they can do the most damage or held back in the aqueous phase is important.

Radiation induced damage to solvent extraction processes was first presented as a topic of potentially serious magnitude at the First International Conference on Peaceful Use of Atomic Energy in 1955 (Schulz 1984). As nuclear fuel was taken to higher burnup and levels of radioactivity, it became increasingly apparent that radiation damage would be a concern. Most radiolysis studies of both TBP and other extraction reagents that have followed since then were carried out using an external gamma ray source. Experimentally this is relatively easy to achieve since the sample need never come into direct contact with the radioactive source material. However, with higher burnup, also comes an increased quantity of alpha emitters. Studies have shown that alpha radiation from extracted plutonium can cause more than 75% of the radiation damage to the solvent/ligand mixture (Stollenwerk 1989). Therefore it is important for a complete understanding, to study alpha radiation. Since the 1980's studies have been performed investigating alpha radiolysis some using a helium ion beam as an alpha source (Ladrielle 1983, Sugo 2009) and others using alpha emitters such as ^{238}Pu and ^{211}At (Kulikov 1983, Lloyd 1985, Kawaguchi 2009, Fermvik 2011, Hui-bo 2012). The helium ion beam technique has the benefit of not leaving a sample radioactive but it faces the challenge of not reaching high doses over short

periods of time, and may not distribute the dose evenly throughout the sample unless there is superb mixing. Using ^{238}Pu has the benefit of being similar to the isotopes found in an actual process. However results reflect the effects of both radiolysis and metal ion catalyzed hydrolysis which requires additional experiments to separate the two (Lloyd 1985). Radiolysis cannot be studied independently from metal ion effects. Additionally, licensing and special equipment are required for dealing with long lived radioactive actinides which may not be readily available in all laboratory settings.

1.3 Proposed method for studying alpha radiolysis: the $^{10}B(n,\alpha)^{7}Li$ reaction

Alpha radiolysis studies can benefit from a method which can produce significant dose rapidly without leaving the samples contaminated with long-lived radioactive isotopes. We have proposed a novel approach, using the well known $^{10}B(n,\alpha)^{7}Li$ reaction currently investigated in such processes as boron neutron capture cancer therapy (BNCT)(Hawthorne 1998) as a means of studying the effects of high LET radiation on solvent extraction processes (Figure 5). It is anticipated that this method can be used as an alternative or complement to helium ion or radioactive alpha isotope studies, as well as a complement to gamma radiolysis studies.

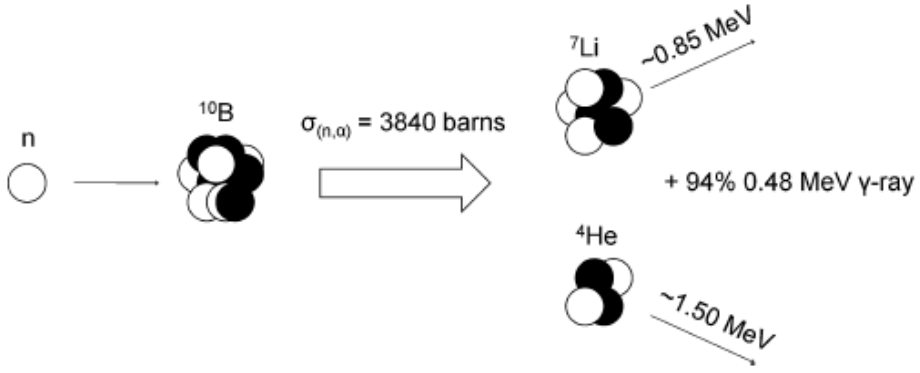

Figure 5. The neutron induced $^{10}B(n,\alpha)^{7}Li$ reaction.

1.3.1 LET considerations

Although the helium or alpha particle and the lithium particle at 1.5 MeV and 0.8 MeV are less than the typical 5 MeV alpha particle emitted from actinides in used nuclear fuel, their LET is similar and should produce very similar effects (slightly above 200 eV/nm for the $^{10}B(n,\alpha)^{7}Li$ reaction vs. ~90 eV/nm for a 5.5 MeV alpha)(LET estimated for alphas of various energies from Figure 6 from (Schuler 1957), Table 6.2 from (Choppin 2002), and Table 1 from (LaVerne 2005)). This can be visualized by observing the response of the aerated Fricke dosimeter in the presence of a variety of sources of radiation and respective LET including gamma radiation, 5.5 MeV alphas, and the $^{10}B(n,\alpha)^{7}Li$ reaction (Figure 6, top trend). The left-most point for gamma at 0.2 eV/nm converts iron(II) to iron(III) at a rate of 1.55 μmol per joule of radiation energy deposited. The two sets of points on the far right correspond to iron(III) formation from 5.5 MeV alphas from ^{210}Po and the $^{10}B(n,\alpha)^{7}Li$ reaction respectively. The response is similar, ~0.55 μmol/J vs. 0.42 μmol/J. This suggests that response from the $^{10}B(n,\alpha)^{7}Li$ reaction to a solvent extraction process should be similar to that from a ~5 MeV alpha source, and that if necessary, a plot similar to that shown in Figure 6 could be created to approximate what a 5 MeV alpha would produce without having to use radioactive isotopes or helium ion beam.

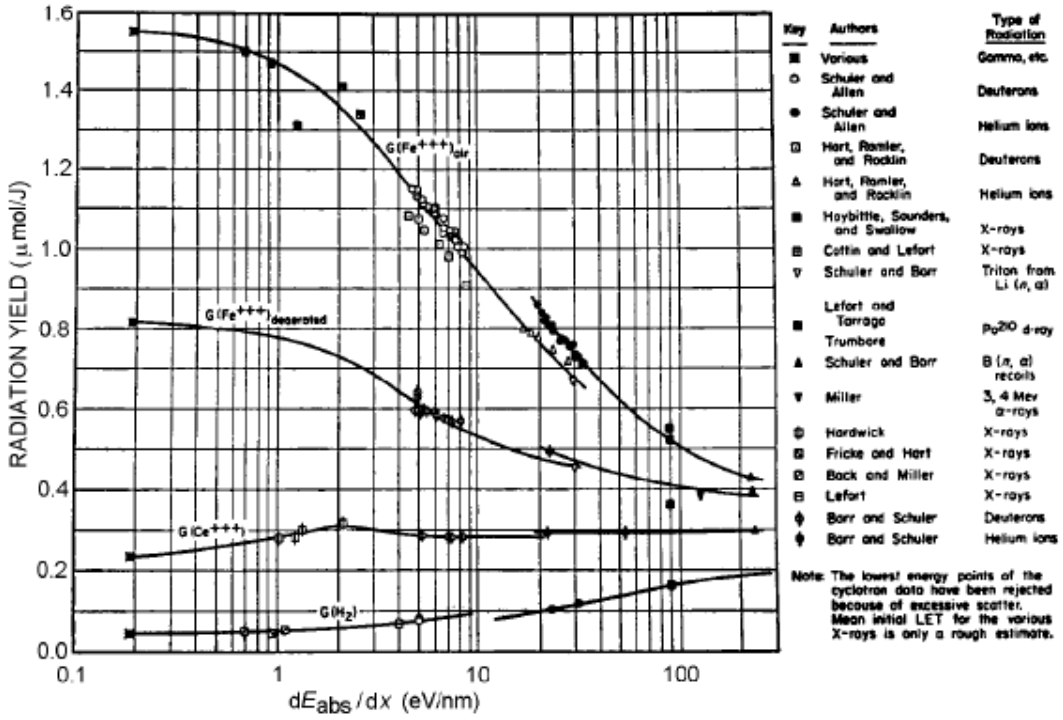

Figure 6. G-Fe(III) and G-Ce(III) for Fricke and cerium dosimeter vs. LET (Reproduced from (Allen 1961)).

1.3.2 Systems and aims of study

The $^{10}B(n,\alpha)^{7}Li$ reaction was implemented as a means to study high LET radiation on solvent extraction processes and apply it as a representation of alpha radiolysis. To gain fundamental insight into the chemistry and mechanisms of reaction and degradation, we studied the solvent under dry and nitric acid contacted conditions, and observed their individual contributions. This method was applied at first to solutions containing dyes for characterization and experience, then to the PUREX TBP solvent for comparison and verification to other published values in the literature, and finally to ligands CMPO and TODGA used for actinide/lanthanide separations. The impacts were quantified by observing the following responses: loss of parent ligand, formation/identification of degradation products, and changes in solvent extraction behavior. These responses can be

modeled as a means of predicting degradation behavior and deriving additional mechanistic insights from degradation constants calculated from the models.

1.3.3 Note on dosimetry

An extremely important factor in carrying out robust radiolysis experiments is performing accurate dosimetry. The Fricke dosimeter (Schuler 1956)(Figure 6) is used here for dosimetry as it is the most widely trusted and utilized dosimeter and has been characterized for both gamma and the $^{10}B(n,\alpha)^{7}Li$ dose (Schuler 1956). This dosimetry is carried out in an aqueous system. For gamma irradiation experiments, dose obtained from the Fricke dosimeter is generally applied directly to organic systems, as dose is related to the number of electrons present which is strongly correlated to mass, interacting with the matter present, independent of density. This assumption is quite typical across the literature and is the best standard for reporting dose and comparing radiolysis studies. For the $^{10}B(n,\alpha)^{7}Li$ reaction, due to the short distance of the alpha particles, it is assumed that all of the alpha dose is absorbed within the sample. Therefore, dose is first characterized per volume for the Fricke system, and then corrected, based on the density of the solvent system being studied. Another minor correction may be made for the difference in diffusion of neutrons in the solvent compared to water, as will be discussed below. Another important consideration when describing the dose and effects of the background radiation from the reactor core is to properly describe the individual dose from the different background components, gamma, beta, and neutron irradiation.

1.4 Modeling degradation

In studies in the literature acid hydrolysis of TBP has been modeled as a series of first order kinetic reactions in an ideal stirred tank environment to predict degradation product formation (Stieglitz 1984, Egorov 2005). Other studies have considered these same equations to model degradation of TBP in the presence of radiation (Kulikov 1983, Vladimirova 1986, Vladimirova 1987, Vladimirova 1989). Such equations can be especially helpful in modeling degradation in a mixed radiation field such as that present in a nuclear reactor. Based on the degradation constants obtained from these fits, equations can be derived representing theoretically pure gamma or high LET radiation, the derivative of which represents the respective G-value of formation or degradation of molecules induced by the individual radiation types.

Gamma induced degradation of TBP can be described by the following equation:

$$C_T = C_{T0} e^{-k_{1\gamma}\dot{D}_\gamma t} \tag{1}$$

$\dot{D}_\gamma$ is gamma dose rate, C_{T0} is the initial TBP concentration at zero dose, $k_{1\gamma}$ is the gamma degradation constant for TBP, and t is time of exposure. $k_{1\gamma}$ can be split into two separate constants $k_{2\gamma}$ and $k_{3\gamma}$ which account for different degradation products of TBP as mentioned above. The constants are related by a simple addition, $k_{1\gamma} = k_{2\gamma} + k_{3\gamma}$.

The concentration of DBP as a function of dose takes into account the formation from TBP degradation (from $k_{2\gamma}$) and the degradation of DBP to all products, represented by $k_{4\gamma}$ in the following equation:

$$C_D = \frac{k_{2\gamma}}{k_{4\gamma} - k_{1\gamma}} C_{T0} \left(e^{-k_{1\gamma}\dot{D}_\gamma t} - e^{-k_{4\gamma}\dot{D}_\gamma t} \right) \tag{2}$$

C_D is the DBP concentration. $k_{1\gamma}$ can be found by fitting Equation 1 to the TBP degradation. Then $k_{2\gamma}$ and $k_{4\gamma}$ can be found by using the value of $k_{1\gamma}$ and fitting Equation 2 to DBP degradation. After the degradation of TBP and formation/degradation of DBP due to gamma radiation was found one can model the TBP and DBP concentration trends in the mixed gamma/high LET radiation environment using Equations 3-4 below. For the sake of simplicity high LET dose and constants are denoted as α in the equations.

$$C_T = C_{T0} e^{-(k_{1\gamma}\dot{D}_\gamma t + k_{1\alpha}\dot{D}_\alpha t)} \tag{3}$$

$$C_D = \frac{\left(k_{2\gamma}\dot{D}_\gamma + k_{2\alpha}\dot{D}_\alpha\right)}{\left(k_{4\gamma}\dot{D}_\gamma + k_{4\alpha}\dot{D}_\alpha\right) - \left(k_{1\gamma}\dot{D}_\gamma + k_{1\alpha}\dot{D}_\alpha\right)} C_{T0}\left(e^{-\left(k_{1\gamma}\dot{D}_\gamma + k_{1\alpha}\dot{D}_\alpha\right)t} - e^{-\left(k_{4\gamma}\dot{D}_\gamma + k_{4\alpha}\dot{D}_\alpha\right)t}\right) \tag{4}$$

2. EXPERIMENTAL

2.1 Gamma irradiations

Gamma irradiations were performed in a cesium-137 gamma cell (CS137 Irradiator Mark-I, Model 68, JL Shepherd & Associates) as a source of gamma rays. Samples were exposed to gamma radiation for different periods of time and at different distances from the center source to achieve a range of doses and dose rates.

2.2 High LET irradiations

For the high LET irradiations the UC Irvine 250 kW TRIGA® Reactor was used as a neutron source to initiate the $^{10}B(n,\alpha)^{7}Li$ reaction as a source of high LET dose. Sample location in the reactor core, reactor power, irradiation time, and concentration of ^{10}B, were varied to provide a variety of doses and dose rates for this study. The TRIGA® reactor is equipped with several sample locations of which two were used (Figure 7), a sample carousel called

the Lazy Susan (LS), and a pneumatic transfer line (PT). The LS is loaded prior to bringing the reactor critical at the desired power, and samples are removed after the completion of the irradiation after the reactor is shut down. Samples in the PT are closer to the center of the core, receive a higher dose relative to the LS at the same power, and may be inserted or removed while the reactor is in operation.

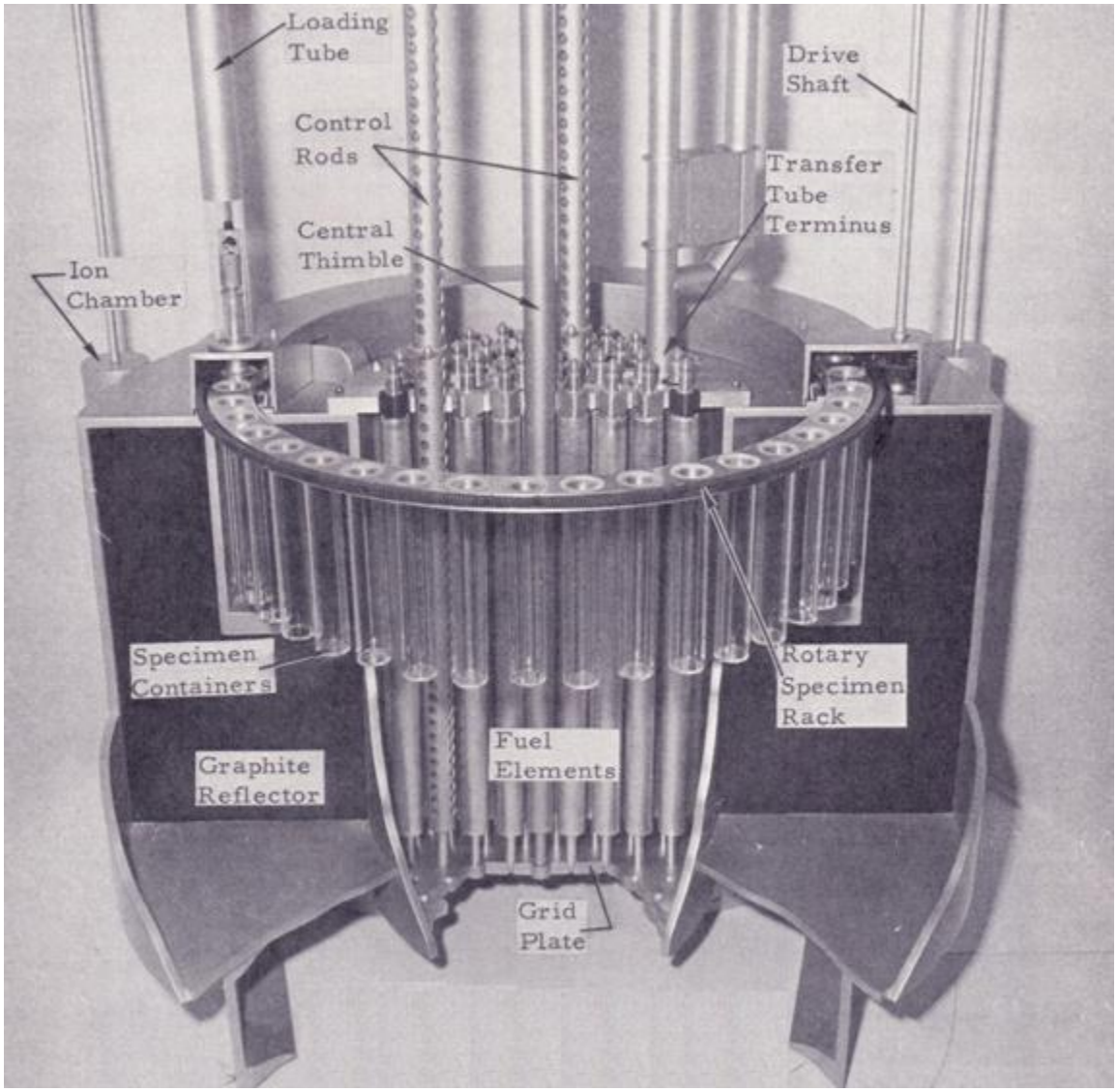

Figure 7. Diagram of TRIGA reactor (GeneralAtomic 1969). The rotary specimen rack which mechanically revolves around the core is fed by the Loading Tube and is termed the Lazy Susan Carousel. The Transfer Tube is fed pneumatically and is termed the pneumatic transfer line.

2.2.1 ^{10}B Sources

A variety of ^{10}B sources were employed throughout this work. Enriched ^{10}B powder (Alpha Aesar) was studied as a possible source for both aqueous and organic solution irradiations. Boric acid (Sigma Aldrich), containing natural boron which is ~20% ^{10}B, was used for aqueous irradiations. Boric acid containing enriched ^{10}B (Sigma Aldrich), and boric anyhydride (Sigma Aldrich) were also used as sources of ^{10}B for aqueous irradiations. Unless specified to contain enriched ^{10}B, mention of boron sources are implied to contain natural boron with ~20% ^{10}B, and dose calculations were always derived based on only the amount of ^{10}B present. The balance of natural boron contains the isotope ^{11}B which absorbs neutrons to a negligible extent due to a low absorption cross section of 0.005 barns compared to 3840 barns for the $^{10}B(n,\alpha)^{7}Li$ reaction. Boric acid enriched in ^{11}B was also used as a control to demonstrate the absence of other interfering chemistry effects from the presence of boric acid.

For organic phase irradiations, molecules were selected that contained boron and were soluble in organic solutions. Solubility is important so that the boron is ensured to be evenly dispersed throughout the sample during the irradiation. These were tributyl borate (Sigma Aldrich), bis(pinacolato)diboron (Sigma Aldrich), decaborane (Sigma Aldrich), carborane (Sigma Aldrich), and ^{10}B enriched carborane (KatChem). A summary of these boron compounds is shown in Figure 8.

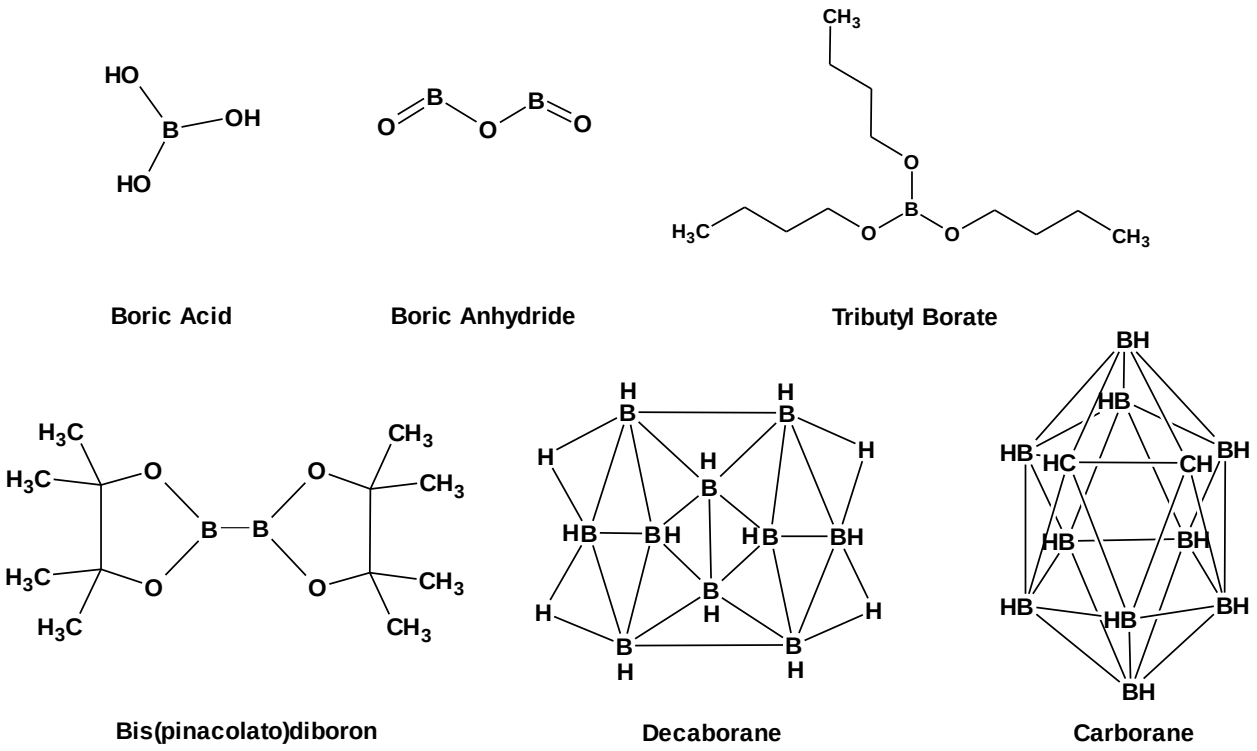

Figure 8. Boron compounds used as a source of ^{10}B for the high LET irradiations.

2.3 Aqueous and organic phase dosimetry

Fricke dosimetry involves the conversion of iron(II) to iron(III) due to energy deposited from radiation in dilute iron solutions containing 1 mM Fe(II), 1 mM NaCl and 0.4 M H_2SO_4. All Fricke solutions were aerated by bubbling air through them for a minimum of 30 min. Calibration standards of varying concentrations of Fe(III) in 1 mM NaCl and 0.4 M H_2SO_4 were prepared. The iron(II) sulphate heptahydrate and ferric ammonium sulphate dodecahydrate (Fe(III)) were both of ACS certified grade and obtained from Fisher Scientific. The sodium chloride was from standardized stock solutions in our laboratory made from filtered and recrystallized NaCl obtained from Fisher Scientific. The sulfuric acid was prepared from concentrated H_2SO_4 (17.8 M) and was obtained from EMD Chemicals.

Gamma induced iron(III) formation was characterized in the cesium irradiator with Fricke solutions containing no boron. Gamma and high LET induced iron(III) formation were characterized in the LS and PT of the TRIGA reactor from samples with and without boric acid. Formation of iron(III) was quantified via measurements in a UV–VIS spectrometer (Ocean Optics JAZ), using 1 cm quartz cuvettes, by observing the characteristic peak at 304 nm. Then iron(III) formation was converted to dose using G-iron(III) values of 1.55 μmol/J and 0.42 μmol/J reported for gamma radiation and the $^{10}B(n,\alpha)^{7}Li$ reaction respectively in the literature (Choppin 2002).

2.4 Organic dyes and analysis methods

Methylene blue (TCI America) and methyl red (Sigma Aldrich ACS Reagent Grade) (Figure 9) were studied at various stages of the project to verify and understand response from the $^{10}B(n,\alpha)^{7}Li$ reaction in a solution on organic compounds. As dyes, these are less stable than typical extraction ligands and analysis via absorption spectroscopy is simple, irradiations can be performed over short periods of time and data can be collected quickly. Methylene blue was studied at 16 μmol/L in water and methyl red was studied at 18 μmol/L in n-dodecane (Acros 99%). Methylene blue in water had a blue appearance and methyl red solutions in n-dodecane were yellow. Degradation based on irreversible bleaching was quantified using UV-VIS spectroscopy. Methylene blue was quantified based on the characteristic peak at 292 nm and methyl red at 456 nm.

Due to the tendency of methyl red to reversibly bleach in the presence of light, special care was taken to shield samples from the presence of light before and during UV-VIS analysis. Significant effort was put into ensuring that an equilibrium was reached and

that this effect did not adversely disrupt the analysis. Methylene blue can adsorb to glass surfaces and special care was taken to ensure that this did not artificially alter concentrations during dilutions or sample preparation and analysis.

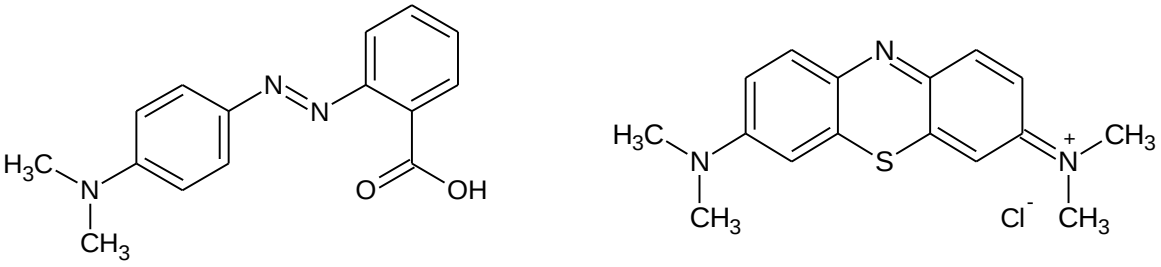

Figure 9. 2-[(4-dimethylaminophenyl)diazenyl]benzoic acid (methyl red), and 3,7-bis(dimethylamino) phenothiazin-5-ium chloride (methylene blue).

2.5 Ligands and analysis methods

Solvent extraction ligands studied were tributyl phosphate ,TBP (Acros, 99%), n-octyl(phenyl)-N,N-diisobutylcarbamoylphosphine oxide, CMPO (Strem Chemicals Inc.), and N,N,N',N'-tetraoctyldiglycolamide, TODGA (Marshallton Labs). All irradiations of these compounds were performed in n-dodecane. DBP (Sigma Aldrich 97%), MBP (MP Biomedicals LLC, no assay provided), and phosphoric acid (SAFC 85 wt% in water) as degradation products of TBP were also purchased and analyzed as standards. TBP and TODGA were analyzed with gas chromatography and CMPO with high pressure liquid chromatography (HPLC).

2.5.1 Gas chromatography

An HP-5890 GC and an Agilent DB-5, 30 m or 15 m length, 0.25 mm inner diameter, and 0.25 μm film thickness capillary columns were used for analysis of parent ligand and respective degradation product analysis. The oven was programmed from 60 ^{o}C to 280 ^{o}C

at a rate of 10 ^{o}C/min. A cool-on-column injection inlet was utilized to eliminate or reduce the possibility of thermal degradation to long chain polymer or low stability degradation products. Detection was performed with a flame ionization detector (FID) for general peak identification and with a flame photometric detector (FPD) with a phosphorus filter to identify compounds containing phosphorus.

The DB-5 is a very standard and robust column. The inner surface of the glass capillary column tube is coated with (5%-Phenyl)-methylpolysiloxane which is in the non-polar class of columns. Generally in gas chromatography, lighter molecules elute first and heavier molecules elute last. Throughout the study we experimented with varying the column type, diameter, length, and film thickness. All of these characteristics affect when a compound will elute from the column. Increasing film thickness can enhance separation while increasing residence time. Decreasing diameter or column length sharpens peaks and increases accuracy while decreasing overall separation of all compounds as everything elutes faster. Altering the film characteristics to a more polar or non-polar variety can interact selectively with specific molecules with similar polarity and change elution time, enhancing separation and dividing peaks that may overlap. In general, for the purposes of this study, the DB-5 column was suitable, and the column length was the only variable that was necessary to change to lower elution times of high molecular weight compounds such as CMPO and TODGA.

Calibrations samples were run three times, once prior to, once in the middle of, and once after analysis of irradiated samples. Irradiated samples were analyzed in a randomized fashion to account for any possible drift effects of the GC. To aid in the analysis of degradation products and standards with phosphate groups, a solution of diazomethane

(Ladrielle 1983) in ethyl ether was added to each sample prior to analysis to derivatize the acidic groups (Figure 10) (diazomethane generator kit (Aldrich), diazald (Aldrich 99%), carbitol (SAFC), ethyl ether (EMD Chemicals and Sigma Aldrich-HPLC grade) and potassium hydroxide (Fisher Scientific)). Without this modification, acid containing molecules exhibit poor volatility, interacting too strongly via the hydroxyl acidic group either with each other or the column surface, resulting in delayed and non-reproducible peaks. Samples were diluted in hexane (Fisher Scientific HPLC grade) for analysis with triphenyl phosphate (Acros 99+%) at 0.5 mmol/L as an internal standard for reference.

2.5.1.1 TBP analysis

Standards of TBP, DBP, MBP, and phosphoric acid were used to determine residence times in the column and develop calibration curves for TBP and DBP. Diazomethane was used to derivatize DBP, MBP, phosphoric acid and any phosphoric acid containing degradation products in irradiated samples (Figure 10). The calibration range covered the experimental concentrations of TBP (0.2 – 1.0 mol/L) and DBP (0.03 – 0.16 mol/L). A dilution of 500x prior to analysis on the FID placed both of these concentration ranges for TBP and DBP in the correct sensitivity range of the FID such that both could be accurately quantified with a single analysis. A dilution of 500x or 5000x was used for the FPD due to its high sensitivity, however these data were used qualitatively for peak location rather than for peak quantification.

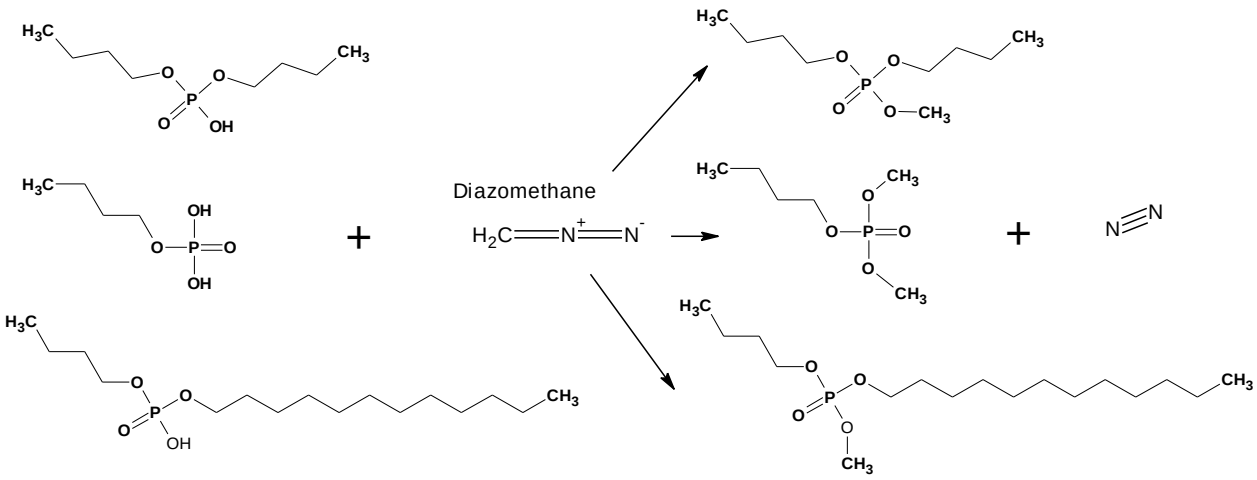

Figure 10. Derivatization with diazomethane. A methyl group is added to the oxygen of an alkyl phosphoric acid replacing the hydrogen and removing acidic properties which are not compatible with GC analysis.

2.5.1.2 TODGA analysis

Due to its high molecular weight (580.98 gm/mol), TODGA was analyzed on the GC with a 15 m DB-5 column as opposed to a 30 m column to allow the molecule to elute faster and avoid degradation at high temperatures. This method proved satisfactory and has been used in the literature for both TODGA (Sugo 2009) and CMPO (Gatrone 1990).

2.5.2 High pressure liquid chromatography (HPLC) analysis of CMPO

Analysis of CMPO was carried out on an HP 1100 HPLC isocratically using a mixture of 30 mM phosphate buffer, pH 2.6, and 2-propanol with 3.6% 1-octanol in 60/40 ratio. A C18 reverse-phase (RP-C18) column (Supelco, 25 cm × 4.6 mm, 5 _m) was used with a flow rate of 1 mL/min. The column temperature was maintained at 50 ^{o}C. The CMPO concentration was determined at a wavelength of 220 nm, based on its UV spectrum. Prior to analysis samples were diluted by a factor of 100 to 1 mmol/L in n-propanol containing 1 mmol/L HPLC grade triphenyl phosphate as an internal standard.

3. RESULTS

3.1 Dosimetry

3.1.1 Gamma cell dosimetry

Figure 11 shows the gamma cell and the various positions for which the gamma or low LET dose rate was characterized. The four sets of large diameter slots with seven separate positions each at increasing distances from the source were analyzed for dose rate with Fricke dosimetry. Figure 12 shows the dose rate in kGy/hr with respect to distance from the source. First iron(III) formation was quantified with UV-Vis and then converted to dose with the G-iron(III) for low LET of 1.55 μmol/J.

Figure 11. Mark-I gamma irradiator cell and sample tray.

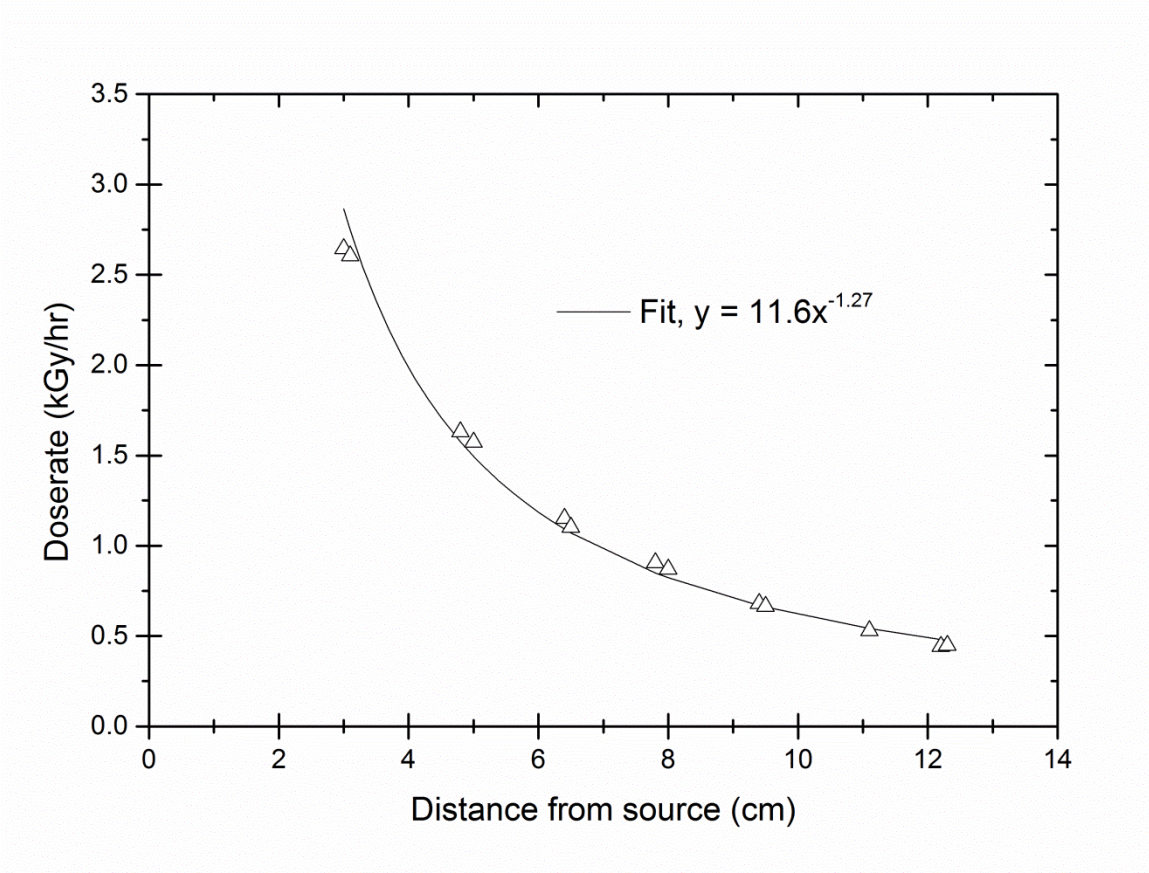

Figure 12. Mark-I gamma irradiator dose rate vs. distance from the cesium source.

3.1.2 Background dose from the TRIGA reactor

In an effort to create an acceptable mixed field kinetic model of degradation it is important to know what type of dose and how much is being received from the reactor itself, prior to addition of ^{10}B for high LET irradiation. Neutron fluxes have been measured previously for the UCI TRIGA® reactor and generic gamma, fast neutron, and thermal neutron doses have been published and scaled to our reactor size as an estimation (Miller 2012). These are summarized in Table 1.

Table 1. Neutron flux in the UCI TRIGA reactor and typical radiation dose rates in the Lazy Susan at 250 kW.

	Gamma/Beta	Fast Neutron	Epithermal Neutron	Thermal Neutron
Flux ($x10^{10}$ $n/cm^2/s$) (Crofoot 1989)	N/A	8.7	6.5	80
Dose (kGy/hr) (Miller 2012)	72	47	N/A	18

Data in Table 2 demonstrate that in a typical TRIGA reactor, the majority of the dose to a sample can be from gamma/beta if the absorbing material has low neutron cross section for high LET reactions such as the $^{10}B(n,\alpha)^{7}Li$ reaction. Neutrons can deposit dose by four main mechanisms. These are neutron absorption n,γ reactions, n,p reactions, neutron decay to protons with 0.8 MeV beta emission, and ejection of protons from molecules as a free proton or combined deuterium atom (must be greater than ~5 eV to break the bond). If the majority of the background radiation is low LET, with an average ≥~1 MeV prompt gamma for fission or neutron absorption (MIT , Pleasonton 1972), it can be lower LET than the 0.66 MeV gammas emitted from ^{137}Cs source which have an LET of 0.39 eV/nm.

Fricke irradiations performed in the LS were used to estimate background dose rate. Assuming that the majority dose is low LET gamma and beta, the value of 1.55 μmol/J was used to convert observed iron(III) formation to dose rate. Original data from the LS (background dose from study in Figure 13 a, c, reactor power 0.5-3 kW) with linear extrapolation to high power suggested a background reactor dose of ~63 kGy/hr at 250 kW. These samples were in the reactor for a short period of time, 7 minutes, and were

exposed to additional radiation during the minutes before and after the irradiation while they were sitting in the LS. This presents a minor challenge due to the large ramp-up time to reach the desired reactor power relative to the short exposure time. This can potentially be overcome by performing irradiations at powers much less than 0.5 kW for longer durations of time, making the ramp-up dose negligible compared to the overall dose. However, this could present an additional challenge because at lower powers, background radiation from fission products of previous runs becomes more relevant to the total dose. Uncertainties at such low reactor power may create uncertainties while extrapolating to dose high reactor power.

An alternative approach to calculate background dose in the LS is to use background dose data collected in the PT and adjust it to the LS based on the ratio of thermal ^{10}B activating neutrons present in the LS vs. the PT. This can serve as a reflection of the difference in background dose coming from the reactor in the two locations. The PT allows rapid entry and retrieval, overcoming challenges at high power with ramp-up dose and the low dose range of the Fricke dosimeter. Results showed a dose rate of ~120 kGy/hr at 250 kW in the PT. Based on Crofoot's measurements (Crofoot 1989) and ^{10}B dosimeter response (section 3.1.3) there is a factor of 2.8 difference in thermal neutrons in the PT vs. the LS. Using this ratio a background dose rate of ~40 kGy/hr is estimated for the LS at 250 kW. It is reasonable to consider thermal neutron flux an acceptable representation of background dose from the core considering Crowfoot's measurements which show that only 10-20% of the neutron population is not thermalized in the vicinity of the PT and LS. Any additional thermalization of neutrons between the PT to the LS is small and the thermal neutron flux can be considered a suitable representation of the fission rate and

overall background radiation coming from the core. Furthermore, agreement between data on methylene blue irradiations in the reactor without boron and the literature for gamma (section 3.3) as well as DBP formation during TBP irradiations in the reactor with no boron and that formed in the ^{137}Cs irradiator (section 3.4.1), corroborates this value. For TBP irradiations, additional insight into the nature of the background radiation from the core, both dose and LET, was helpful in the interpretation of the results.

3.1.3 High LET dosimetry in the TRIGA reactor

High LET irradiations were carried out in the LS and PT utilizing high LET particles He^{2+} and Li^{x+} from neutron activation of ^{10}B via the $^{10}B(n,\alpha)^{7}Li$ reaction. We therefore set out to collect data from which we could derive a correlation useful for estimating high LET dose based on the concentration of ^{10}B present in solution, and flux of neutrons (reactor power). As discussed, a method for quantifying high LET dose by spectrophotometrically measuring iron(III) formation due to ^{10}B (boric acid) activation in a Fricke Dosimeter placed in a neutron field has been described (Figure 6, (Schuler 1956)).

Aqueous Fricke solutions containing 0–0.9 M boric acid were prepared for irradiation. Boric acid containing a natural abundance of the ^{10}B and ^{11}B isotopes served as the source of ^{10}B for the $^{10}B(n,\alpha)^{7}Li$ reaction. Approximately 1.5 mL of this solution was added to 1.5 x 5 cm sealed polyvials. Different sample sets were irradiated in the LS at 0.5, 1, 2, and 3 kW, respectively for 7 min. The estimated thermal neutron flux in the carousel positions is 3×10^{9} neutrons/cm^2 at 1 kW.

Fricke solutions containing 0 M to 0.32 M boric acid were also prepared and 1 mL added to smaller 1 x 2 cm polyvials for irradiations in the PT. These samples were

transferred into the reactor core operating at critical powers of 10, 50, 100, 150, and 250 kW for durations of 2.5 min, 30, 15, 9, and 9 s respectively. The estimated thermal neutron flux in the PT is 2.2 x 10^{12} neutrons/cm2 at 250 kW (Crofoot 1989). These additional irradiations were performed to evaluate the efficacy of our model over the entire range of power of the UC Irvine TRIGA® reactor and also provide data for the reactor core PT position. High power Fricke irradiations needed to be performed in the PT since at high power, levels of Fe(II) in the Fricke dosimeter are consumed very rapidly. The PT allows for quick entry and removal of samples to and from the core (*2 s transfer time) for short irradiation times of 5 min or less.

Post exposure UV Vis analysis of iron(III) formation and dose estimation are shown in Figures 13-14. A set of non-irradiated samples were analyzed as blanks. Irradiated solutions containing no boric acid were analyzed to correct for iron(III) formation due to background gamma and neutron radiation from fission and decay products in the core. Iron(III) formation from these blanks was subtracted from raw mixed data (Figure 13 a,b) to derive iron(III) formation from the $^{10}B(n,\alpha)^{7}Li$ reaction only (Figure 13 b,c). Solutions containing boric acid were also irradiated in a ^{137}Cs gamma Irradiator to confirm that the low LET G value of iron(III) formation during gamma irradiation is not affected by the boric acid present in the sample.

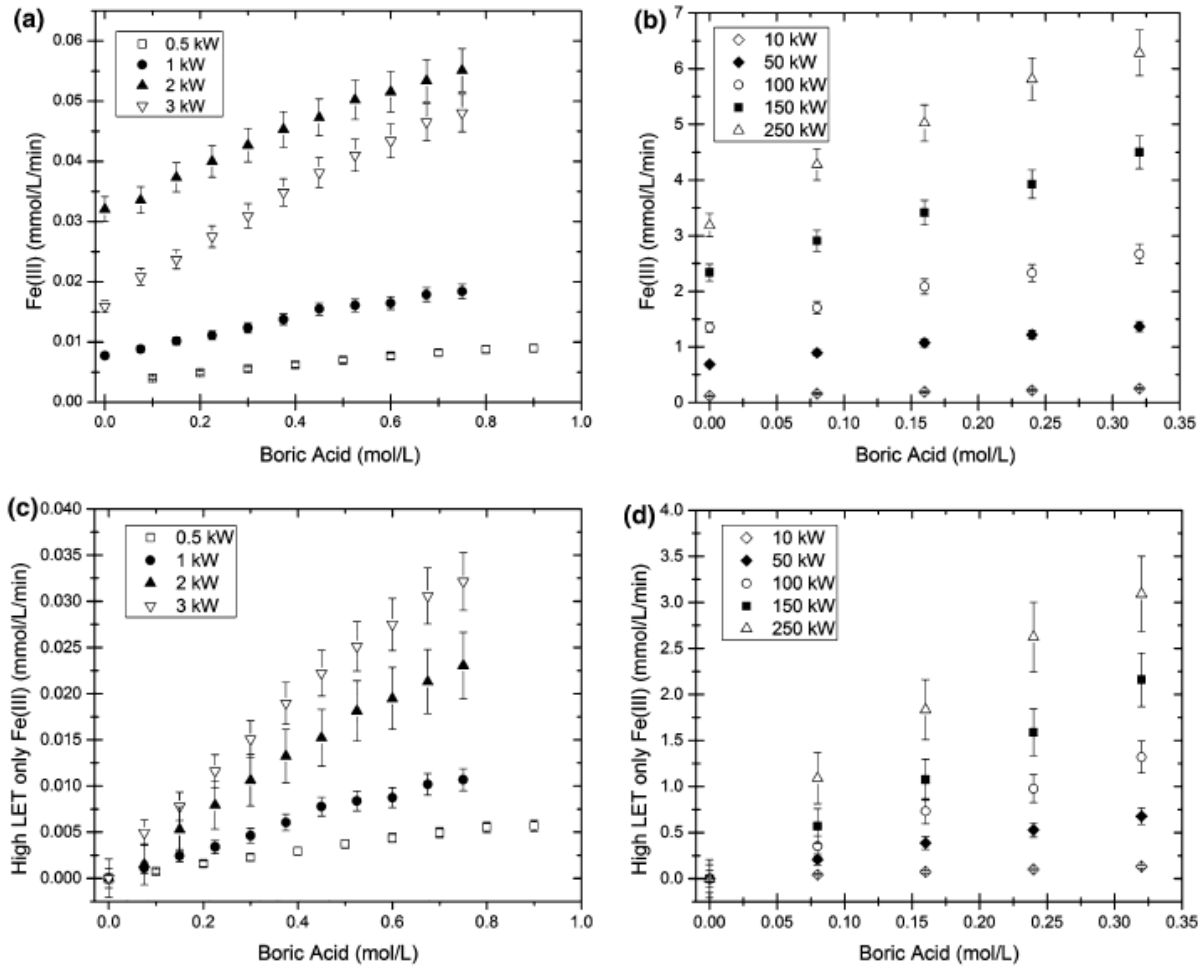

Figure 13. Total iron(III) formation in samples with boric acid irradiated at various times and reactor power. a) LS results. b) PT results. c) LS results, background iron(III) removed. d) PT results, background iron(III) removed. Error bars are one standard deviation calculated from variations in the triplicate measurements in the UV–Vis spectrometer and estimated variations in irradiation times. LS data reproduced from Pearson and Jan et al. (Pearson J. 2013) with permission from Springer.

The value of 0.44 μmol/J reported by Schuler and Barr (Schuler 1956) was used to convert observed iron(III) formation to high LET dose rate and results at each location, LS and PT, are normalized to power and overlaid for better comparison to the correlation or model (Figure 14 and Section 3.1.3.1).

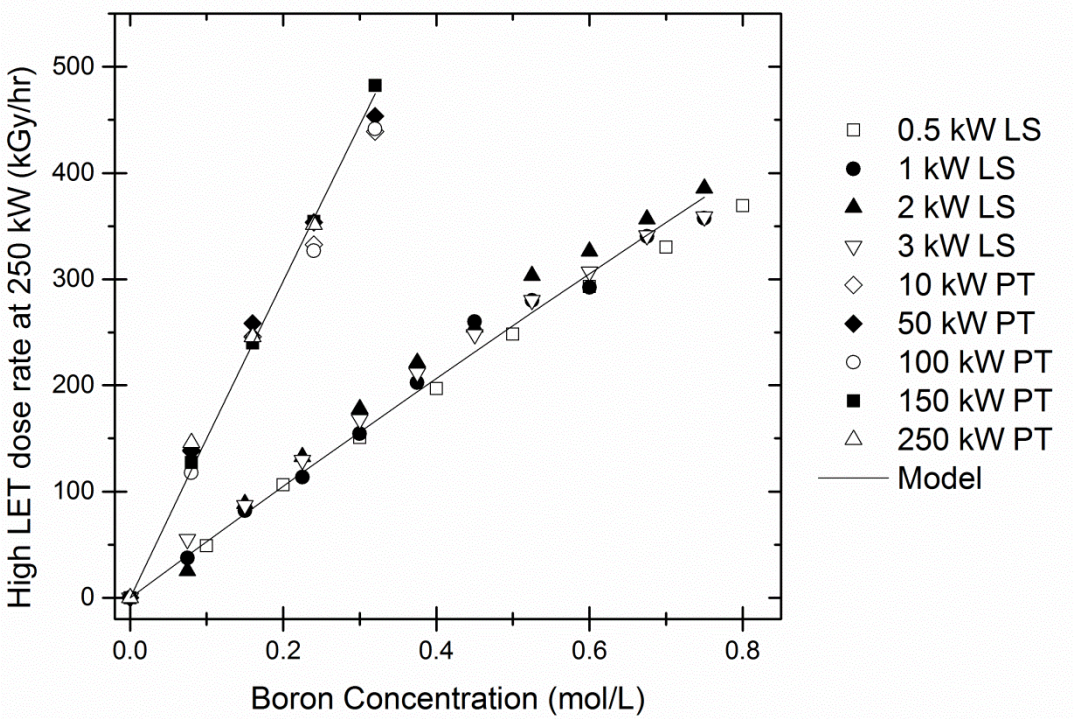

Figure 14. High LET dose rate to aqueous solutions versus boron concentration calculated by Eq. (8) for the LS and PT at 250 kW. Adjusted data included to demonstrate fit. Boron concentration reflects boron containing natural abundance of ^{10}B and ^{11}B isotopes. Data reproduced from Pearson and Jan et. al. (Pearson J. 2013) with permission from Springer.

3.1.3.1 Modeling High LET dose in the TRIGA reactor

A slight tapering of high LET dose is observed in Figure 13 and 14 as boron concentration increases. This may be due to ^{10}B self shielding as the atoms come closer to one another (Schuler 1956) or potentially a simple exponential decrease as iron(III) is consumed. Two models were considered to describe this phenomenon, a simple directional exponential attenuation model (Eq. 5) where neutron flux decreases from one side to the other and a solution to a more complex differential equation describing diffusion and absorption within a symmetrical sea of neutrons (Eq. 6-7) where neutron flux decreases towards the center of the sample(Lamarsh 2002). This latter approach takes into account the fact that a significant portion of neutrons leaving the core and passing through the LS and PT will be reflected back by graphite reflectors and moderator. ΔN is the number of neutrons

absorbed, S is the sample surface area on the surface facing the flux (Eq. 5 only), x is the distance from one end of the sample to the other in the direction of flux (Eq. 5 only), t is the time of irradiation, σ_B is the ^{10}B cross section for absorption of neutrons, N_B is the total number of ^{10}B atoms in the sample, and Φ is the neutron flux. Index 0 indicates the flux at the sample surface. r is the sample radius (from r = 0 (center) to r = R (surface)), z is the height of the sample (from z = -H/2 to z = H/2, i.e. z = 0 is the center of the sample and H is the total height), D is the thermal neutron diffusion coefficient (Eq. 6 and 7 only).

$$\Delta N = \phi_o S t (1 - e^{-\sigma N_t x}) \tag{5}$$

$$\frac{1}{r}\frac{\partial}{\partial r}\left(D\, r \frac{\partial \phi}{\partial r}\right) + \frac{\partial}{\partial z}\left(D \frac{\partial \phi}{\partial z}\right) - N_B \sigma_B \phi = 0 \tag{6}$$

$$\Delta N = \int_0^z \int_0^\theta \int_0^r t \sigma_B N_B \phi(r, z)\, r dr d\theta dz \tag{7}$$

While the experimental conditions likely lie somewhere in-between these two idealized representations, it was assumed that the conditions lie closer to the "sea of neutrons" scenario, and these equations were used to model neutron absorption and high LET dose. This is a much more challenging approach since there is no analytical solution to Eq. (6) and the solution must be found numerically. An analytical solution to Eq. (6) cannot be found due to either inhomogeneity of the boundary condition or a nonseparable equation which results if the boundary condition is homogenized. Therefore a numerical solution was sought using the finite element method in the PDEtoolbox™ add on to Matlab®. PDEtoolbox™ can solve a partial differential equation (PDE) that is 2-D in space, e.g. r and z. Our samples are contained in cylindrical vials so this required using the 3-D elliptic PDE problem represented by Eq. (6), and reducing the problem to 2-D using

coordinate transformation in order to draw it and solve it in PDEtoolbox™. The solution to Eq. (6) for flux and corresponding mesh were exported from the PDEtoolbox™ into the Matlab® command window and interpolated into a function U(r,z) using the TriScatteredInterp functionality to solve for ΔN (Eq 7). Then incorporating the iron(III) formations observed (Figure 13) and the G-iron(III) of 0.44 μmol/J, dose can be calculated by Equation 8:

$$High\ LET\ Dose\ (Gy) = \frac{\Delta N E_B}{\rho V} \qquad (8)$$

E_B is the high LET energy of the He^{2+} and Li^{x+} ion from each $^{10}B(n,\alpha)^{7}Li$ reaction, i.e. 2.35 MeV. With the solution to neutron diffusion and absorption, a flux profile can be visualized for a cylindrical sample. Figure 15 shows the variation in flux from the surface to center of a 2-D cross section of the 0.075 - 0.75M boric acid 3kW sample (Lazy Susan) from r = 0 to r = R = 0.7 cm and z = -H/2 to z = H/2 where H is the height of the sample, 0.97 cm.

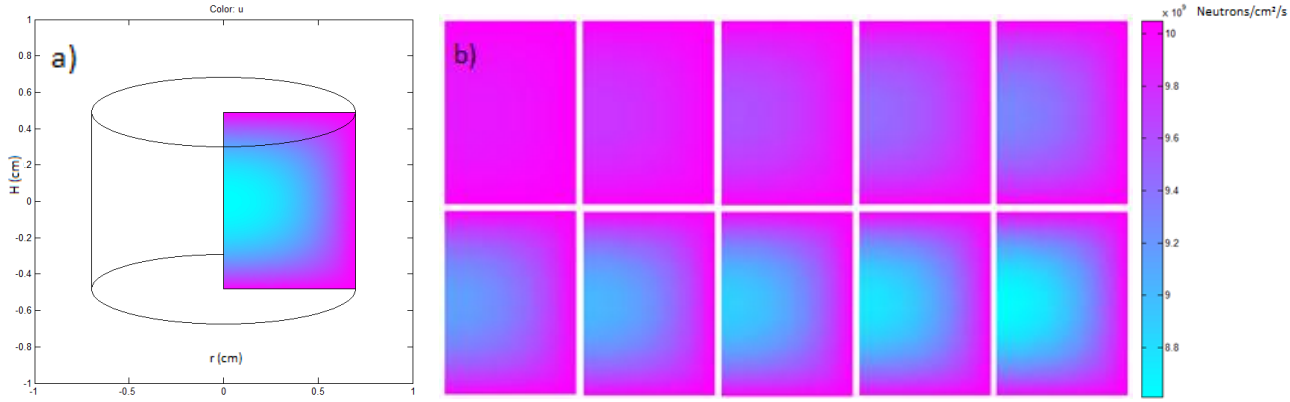

Fig. 15. Flux profile solution calculated in PDEtoolbox™ for samples at 3 kW in the Lazy Susan. a), Profile from sample center to sample surface (r = 0.7 cm), sample cylinder shape added for clarity, 0.75M boric acid. b), Sample profiles from top left to bottom right at 0.075, 0.15, 0.225, 0.3, 0.375, 0.45, 0.525, 0.6, 0.675, and 0.75 M boric acid, note slight decrease in flux (from ~$10x10^9$ to ~$8.6x10^9$ n/cm²/s) as the sample center is approached. Data reproduced from Pearson and Jan et. al. (Pearson J. 2013) with permission from Springer.

Both models (equation 5 and 6) fit the data well at low ^{10}B concentrations as the dose response trend is near linear. It is left to be shown in future experiments if the models

can represent the data well at higher ^{10}B concentrations. It has also been suggested that Monte Carlo N-Particle Transport Code (MCNP), a software package developed at Los Alamos National Laboratory for simulating nuclear processes, may provide an accurate representation of neutron flux and absorption within a sample in the LS. Models such as these will become increasingly important for experiments that are performed at much higher boron concentrations with much more curvature from shielding is present.

At the range of ^{10}B concentrations examined, a reduction in the neutron flux of only ~10% occurred towards the center of the sample (Figure 15). Therefore applying this method to observe the effects of high LET radiation provides a much more even distribution of dose compared to helium ion irradiation where the effects can be localized on the surface of the sample. It is also assumed due to the short travel of the alpha particles, ~50 μm for a 5 MeV alpha particle (Choppin 2002), that all of the dose from the alpha particle is absorbed within the sample.

3.2 Methyl Red Irradiations

3.2.2 Gamma Irradiations

The methyl red structure is shown in Figure 9. Methyl Red solutions were irradiated at various distances from the ^{137}Cs-source for 0–30 h and samples were retrieved and measured with a UV–VIS spectrometer. A near linear decrease in methyl red concentration was observed with increasing dose. A G-value of -4.66E-4 μmol/J was calculated for degradation of methyl red in the presence of gamma radiation (Figure 16).

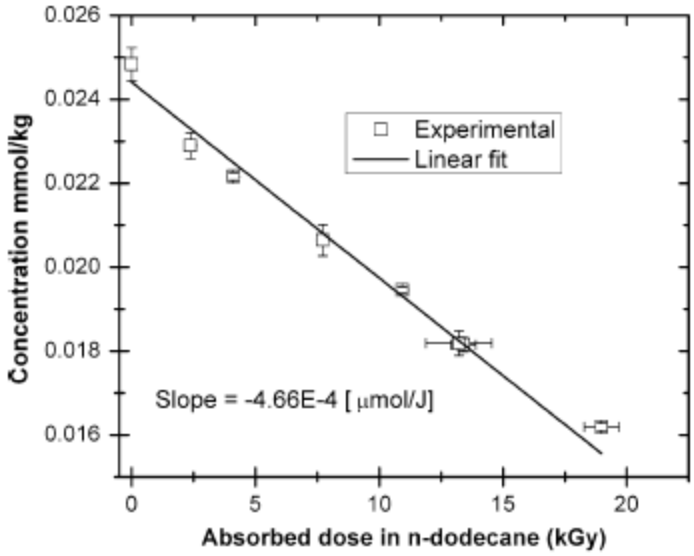

Figure 16. Decrease in methyl red concentration as a function of dose to n-dodecane. The absolute value of the slope reflects the G-value for degradation of methyl red in n-dodecane and the value is given in this figure ($4.66 \times 10^{-4} \pm 0.23 \times 10^{-4}$ μmol/J) Data reproduced from (Pearson 2012) with permission from Springer.

3.2.2 High LET Irradiations

Due to the insolubility of boric acid in organic solutions an alternate compound was sought as a source of boron to produce the $^{10}B(n,\alpha)^{7}Li$ reaction. The first candidate, boron powder was investigated. The powder could be evenly distributed within an organic sample by placing the powder in a plastic irradiation vial and filling the vial up to the height of the powder with methyl red/n-dodecane solution until all the powder is wetted, submerged, and bubbles removed. There was initially concern that this would not prove effective as shielding would be worse in these particles and He^{2+} and Li^{x+} ions released would be trapped within the particles, unable to deposit their energy into the solution. Therefore, this concept was first characterized with Fricke solution for comparison to results in section 3.1.3. Low iron(III) formations with boron powder compared to that observed in Fricke solutions with boric acid confirmed that use of boron powder would not serve as a suitable source of ^{10}B and the $^{10}B(n,\alpha)^{7}Li$ reaction.

This led to the determination that an organic soluble compound should be used, and tributyl borate was selected, which worked exceptionally well as a ^{10}B source. A very minor shift in the UV Vis absorbance peak towards the longer wavelength infrared light was observed which was possibly due to damage to the solution or interaction of methyl red with butyl boric acid compounds formed during irradiation. This shift to absorbance of infrared light would cause higher energy red light to be reflected and blended with the customary yellow appearance of methyl red in n-dodecane, creating an orange appearance which was visually observed. The peak shift did not negatively impact the peak absorbance maximum used for quantifying methyl red concentration and overall tributyl borate did not interfere with collection of satisfactory data via UV Vis analysis.

Methyl red solutions with varying concentrations of tributyl borate from 0 – 0.9 mol/L were put in sealed containers and placed in the LS next to the core of the UC Irvine 250 kW TRIGA_ reactor. Different sample series were irradiated at 10 kW for 3 hr, 30 kW for 1 hr, and 30 kW for 3 hr. Methyl red solutions with no tributyl borate were irradiated to estimate the contribution from low LET dose to the samples as performed similarly with the Fricke solutions dose studies. A set of samples were left outside the core during the irradiations to serve as blanks. After the irradiation the samples were recovered from the lazy-susan and analyzed for an absorbance decrease in the methyl red peak maximum at 456 nm by UV–VIS spectrometry as described above. Methyl red solutions containing tributyl borate were also irradiated in the ^{137}Cs cell to observe if the G-value for methyl red degradation would be affected by the tributyl borate present in the sample and no adverse interaction was observed. Results in Figure 17 show near linear net decrease in methyl red

concentration with increasing high LET dose at a rate of 3.0E-5 µmol/J, fifteen times below that observed for gamma or low LET radiation.

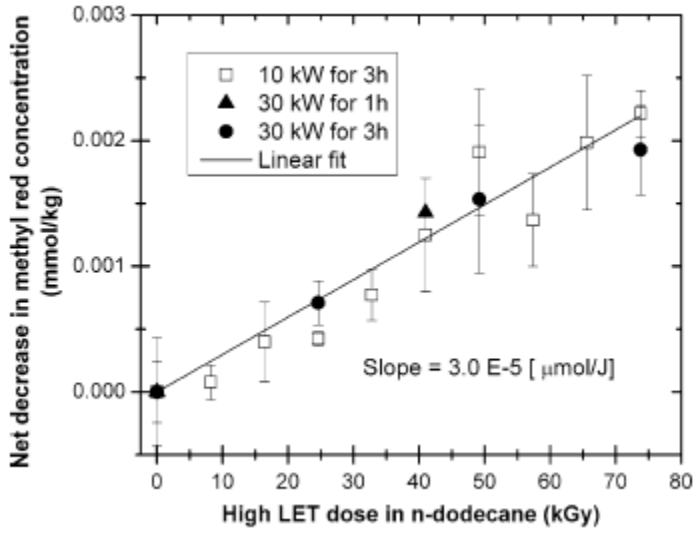

Figure 17. Net degradation of methyl red versus dose rates in kGy for high LET radiolysis at various reactor powers. Error bars are from standard deviations calculated from triplicate samples. Slope reflects the G-value for degradation of methyl red in n-dodecane and the value is given in this figure ($3.0 \times 10^{-5} \pm 0.1 \times 10^{-5}$ µmol/J). Data reproduced from (Pearson 2012) with permission from Springer.

3.3 Methylene Blue Irradiations

16 µmol/L solutions of methylene blue in water with no boron, 0-0.18 M ^{10}B enriched boric acid (0.9 mol/L natural boron boric acid equivalent), and 0.3 mol/L boric anhydride (0.6 mol/L natural boron) were irradiated at 2.5 kW for 5 min, 3 min, and 1.5 min in the reactor PT and analyzed post irradiation with UV Vis spectroscopy. Samples containing 0.18 mol/L ^{11}B enriched boric acid were also irradiated for comparison to samples with no boron and with ^{10}B enriched boric acid to verify that boric acid containing the ^{11}B isotope had a negligible effect on the irradiation results. Samples containing no boron irradiated in the reactor were analyzed as gamma irradiated samples per the characterized background low LET dose rate of 40 kGy/hr/250 kW. Results are shown in Figure 18.

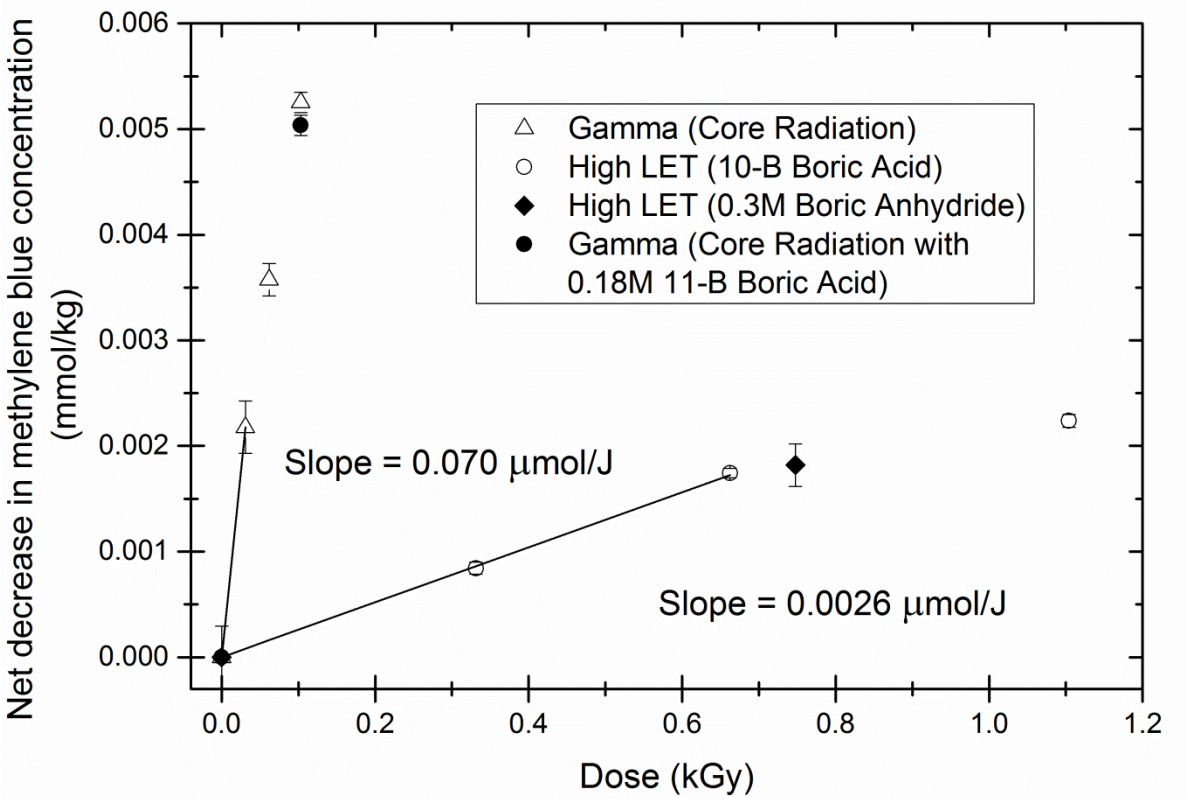

Figure 18. Irradiations of 16 µM methylene blue in the reactor at 2.5 kW with and without ^{10}B containing molecules. Samples without ^{10}B represent low LET radiolysis from background radiation and background radiation has been subtracted from samples which do contain ^{10}B to reflect high LET radiation only. Error bars are from standard deviations calculated from triplicate samples. Slope reflects the G-value for degradation of methylene blue in aqueous solution and the values are given in this figure (0.070 ± 0.008 µmol/J and 0.0026 ± 0.0001 µmol/J for low and high LET respectively).

From data in Figure 18 a G-value of about -0.070 µmol/J is calculated for net methylene blue degradation which shows excellent agreement with work by Jay LaVerne (LaVerne 2005) who found a G-value of -0.074 µmol/J. Irradiation of samples with enriched ^{11}B boric acid only, lie on the trend of those irradiated without boric acid and demonstrate that neither the presence of boric acid nor ^{11}B activation interfere with the high LET radiolysis studies. For the high LET irradiations, results from experiments with boric anhydride also fall on the same trend within error as the experiments with ^{10}B enriched boric acid demonstrating that alternate boron containing compounds yield the same results, and that ^{10}B activation alone is the source of the observed response.

The G-value for methylene blue degradation for the $^{10}B(n,\alpha)^{7}Li$ reaction of 0.003 μmol/J is less than that reported by LaVerne et al., 0.006 μmol/J for 2, 5, and 10 MeV He^{2+} ions, however there is a possibility that these differences may be described by differences in LET. This will be discussed more below. More important is the observation that for both methylene blue, and methyl red, the G-values for degradation were suppressed for high LET radiation compared to low LET radiation. This is attributed to a higher degree of consumption/neutralization of reactive products within the tracks for high LET radiation compared to low LET, which reduces the amount of indirect degradation with respect to dose caused by these reactive products.

3.4 Tributyl Phosphate Irradiations

Preliminary tests were performed to become acquainted with operation of the GC and analyzing TBP and derivatized degradation products in irradiated TBP solutions. It was immediately observed that the tributyl borate was consistently associated with significant and abnormal tailing which made it impractical to quantify and appeared to adversely affect column life and quality. Bis(pinacolato)diboron was chosen as an alternate boron containing molecule soluble in organic solutions for high LET irradiations. It was found to be easily quantifiable with superior stability characteristics, and did not interfere with the GC analysis.

3.4.1 Gamma Irradiations

Solutions of 1 mol/L (M), i.e. 1.23 mol/kg, tributyl phosphate in n-dodecane were irradiated for 33 days in the gamma source receiving doses doses from 381 kGy to 2035

kGy. Concentration profiles of TBP and DBP relative to gamma dose are shown in Figure 19. To verify that bis(pinacolato)diboron did not interact with TBP or DBP and either suppress or enhance their degradation during the reactor irradiations, solutions of 1 M TBP and 0.3 M bis(pinacolato)diboron in n-dodecane and solutions of 1 M DBP and 0.2 M bis(pinacolato)diboron in n-dodecane were irradiated in the gamma source for comparison to each other and to non-irradiated controls (Figure 19 and Figure 20). All samples were visually inspected post irradiation for crud formation or precipitation. Bis(pinacolato)diboron concentrations were measured by gas chromatography (GC) before and after irradiation.

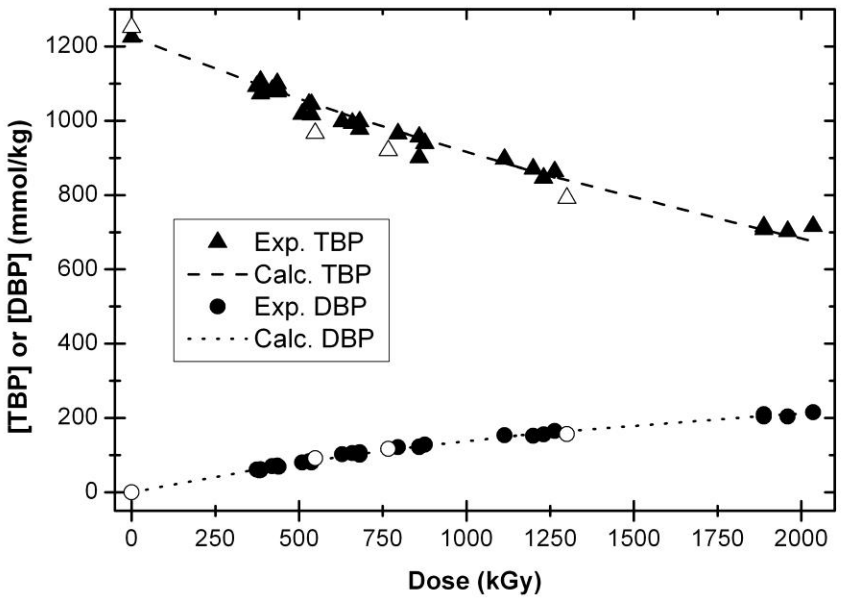

Figure 19. Gamma irradiation of 1M TBP in n-dodecane. Experimental data for the degradation of TBP and formation of DBP with respect to gamma dose are shown as circles and triangles. The lines show the calculated degradation and formation of TBP and DBP using equations 1 and 2, respectively, and decay constants in Table 2 as discussed below. Also shown, as open points, are the results from gamma irradiation of 1 M TBP in n-dodecane in the presence of 0.3 M bis(pinacolato) diboron. Data reproduced from Pearson and Nilsson (Pearson 2014) with permission from Taylor and Francis.

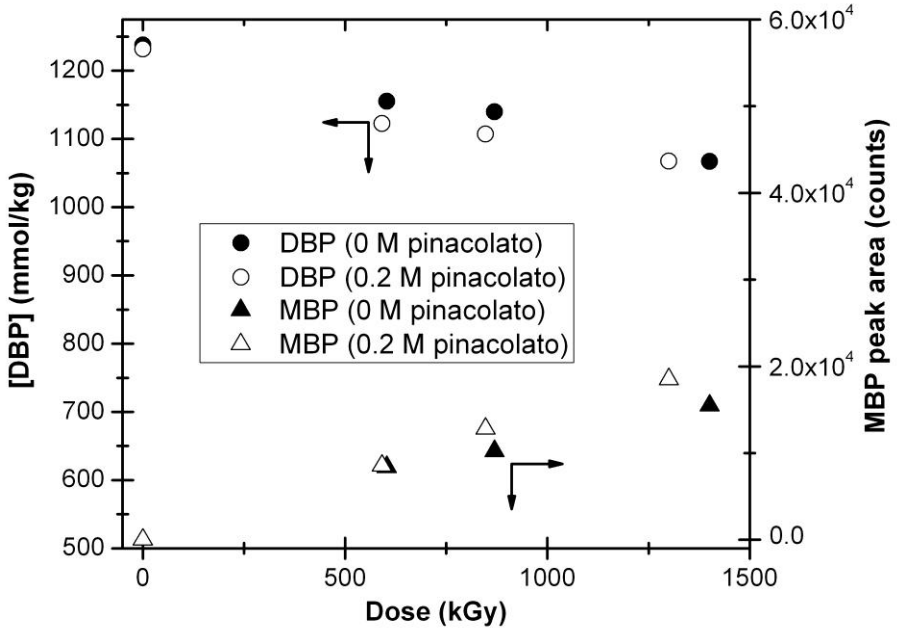

Figure 20. Gamma irradiation of DBP in the ^{137}Cs source in the presence of bis(pinacolato) diboron. Degradation of DBP and formation of MBP with respect to dose. Note the difference in scale for DBP (left side) versus MBP (right side). Data reproduced from Pearson and Nilsson (Pearson 2014) with permission from Taylor and Francis.

It can be seen that the DBP formation due to gamma radiation in solutions of 1 M TBP/n-dodecane with bis(pinacolato)diboron is unchanged compared to solutions without the boron compound. Comparing DBP and MBP in 1M DBP solutions with or without bis(pinacolato)diboron irradiated in the cesium source shows a good match, suggesting the presence of bis(pinacolato)diboron does not affect the degradation by gamma radiation, see Figure 20. Note that the MBP in Figure 20 is reported in total peak area owing to the fact that no standard sample of MPB was available. However, the peak areas were adjusted using an internal standard and are internally consistent showing that MBP formation during gamma radiation is not affected by the presence of bis(pinacolato)diboron. No

precipitation was observed in any of the samples indicating that the bis(pinacolato)diboron remained soluble.

3.4.2 High LET Irradiations

Solutions of 1 M TBP in n-dodecane with bis(pinacolato)diboron ranging in concentrations of 0-0.35 M were irradiated in the UC Irvine TRIGA® reactor at 250 kW for 10 hours. The result from this irradiation is shown in Figure 21. Low LET background dose of 404 kGy received throughout the irradiation from the reactor is noted by the sample which did not contain bis(pinacolato)diboron. In this sample there is a decrease in TBP from 1.23 mol/kg to 1.11 mol/kg and formation of 69 mmol/kg DBP. All samples received the same background dose while samples with bis(pinacolato)diboron received high LET dose up to 4370 kGy for the samples with the highest amount of boron present.

GC analysis showed that up to 50% of the bis(pinacolato)diboron degraded during the irradiations however visual inspection of the samples post irradiation revealed no precipitation. Therefore it was assumed that degradation products of bis(pinacolato)diboron remained soluble, evenly distributed within the samples, and available to absorb neutrons and deposit high LET dose throughout the irradiation. Consumption of boron-10 due to activation was also calculated to have a negligible effect on reducing boron-10 concentrations.

Finally, temperature studies indicated that the temperature in a sample containing 0.15 M bis(pinacolato)diboron in 1 M TBP/n-dodecane irradiated in the lazy susan increased over time but stabilized at about 31 ^{o}C after ~1 h of the reactor irradiation at full power. This difference could speed up degradation rates relative to room temperatures

however the effect is very small and given the good match for the gamma-only effects in the reactor compared to that of the cesium-137 studies (see discussion below) the temperature effect is likely negligible.

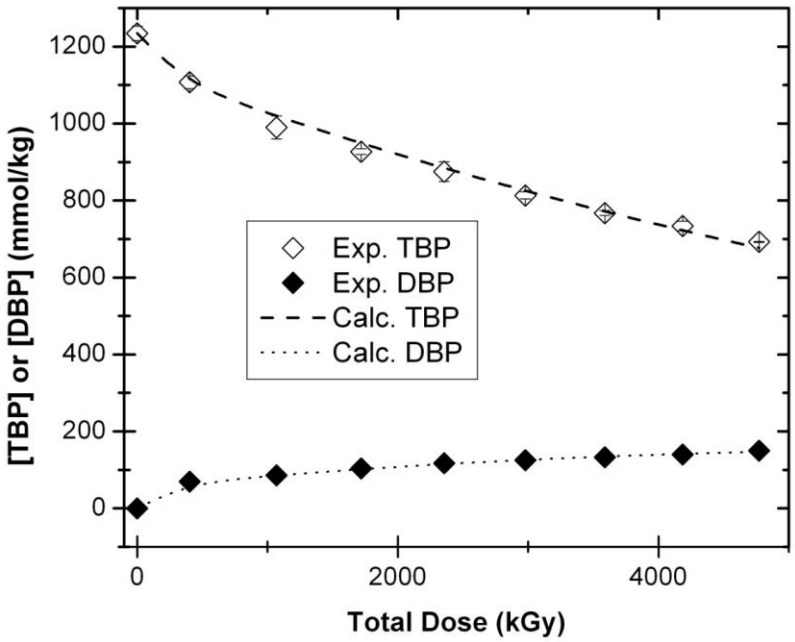

Figure 21. Degradation of TBP and formation of DBP in solutions of 1M TBP in n-dodecane due to dose from low LET in the lazy-susan irradiation position and from high LET irradiation by varying concentrations of bis(pinacolato)diboron. The points at 0 M bis(pinacolato)diboron reflect low LET radiation only (404 kGy). Data reproduced from Pearson and Nilsson (Pearson 2014) with permission from Taylor and Francis.

3.4.3 TBP low and high LET G-Value and degradation constant calculations

For TBP a robust study with multiple data points made it possible to attempt a theoretical fit to the data based on equations 1 - 4 to more accurately describe the degradation. Equations 1 - 4 were fit to the data in Figures 19 and 21. In both fitting routines the sum of chi-squares was minimized by varying the decay constants.

The values for the constant and the errors are shown in Table 2. Taking the derivative of the concentration profile with respect to dose, the instantaneous G-values at low dose are calculated for pure α or γ radiolysis of TBP (Table 3).

Table 2. Degradation constants for TBP and formation of DBP for gamma and high LET radiation. Reproduced from Pearson and Nilsson (Pearson 2014) with permission from Taylor and Francis.

Reaction path	**Constant**	**This Study, (*1E-4 kGy^{-1})**	
		***i* = γ**	***i* = α**
Degradation of TBP to all products	k_{1i}	2.92 ± 0.23	1.11 ± 0.08
Degradation of TBP to DBP, i.e. formation of DBP	k_{2i}	1.48 ± 0.04	0.35 ± 0.01
Degradation of TBP to products other than DBP	k_{3i}	1.44 ± 0.27	0.75 ± 0.09
Degradation of DBP to all products	k_{4i}	2.49 ± 0.48	1.08 ± 0.13

[a]Corresponds to polymer product only

Table 3. G^-_{TBP} and G^+_{DBP} values for gamma and high LET irradiated 1M TBP in n-dodecane extrapolated to zero dose. Reproduced from Pearson and Nilsson (Pearson 2014) with permission from Taylor and Francis.

	Extrapolated to zero dose
$G^-_{TBP\gamma}$, Degradation of TBP by gamma radiation	0.36 ± 0.03 µmol/J
$G^-_{TBP\alpha}$, Degradation of TBP high LET radiation	0.14 ± 0.01 µmol/J
$G_{DBP\gamma}$, DBP accumulation due to gamma radiation	0.18 ± 0.01 µmol/J (G^+_{DBP})
$G_{DBP\alpha}$, DBP accumulation due to high LET radiation	0.043 ± 0.001 µmol/J (G^+_{DBP})

3.4.4 Presence of multiple products in addition to DBP

From data in Table 3 and Table 4 it is immediately apparent that there are a significant amount of alternative products that are formed in addition to DBP. These are best visualized by viewing a chromatogram and analyzing the peaks with the frame of reference described in Figure 3 (All compound elution times reference as numbers have the units of minutes).

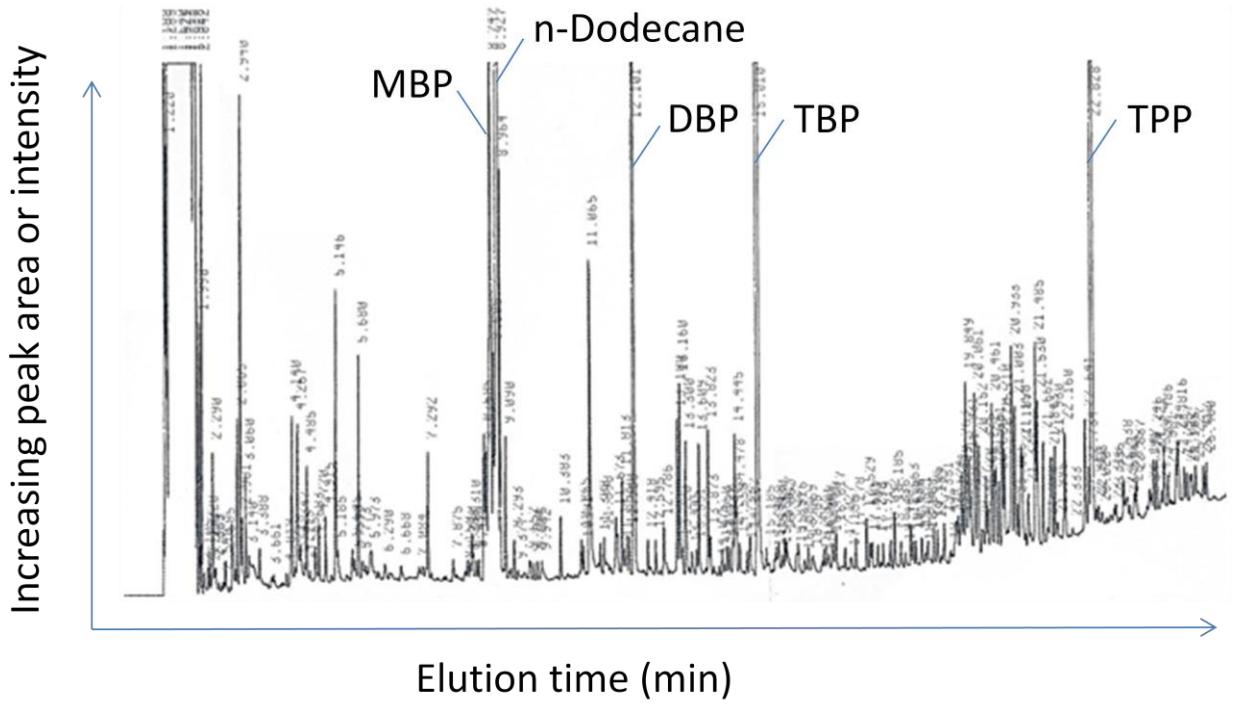

Figure 22. FID GC chromatogram of 1M TBP post gamma irradiation. Note major peaks for MBP (8.747), n-dodecane (8.927), DBP (12.101), TBP (15.010), and internal standard triphenyl phosphate (22.828).

Figure 22 shows a raw FID GC chromatogram of a solution of 1 M TBP/n-dodecane post gamma irradiation. Easily observed are the peaks for MBP (8.747), n-dodecane (8.927), DBP (12.101), TBP (15.010), and internal standard triphenyl phosphate, TPP, (22.828) which were confirmed with standards. Additional peaks represent degradation and recombination products of TBP, DBP, and n-dodecane. The highest probability products of TBP are DBP (an acid), or combination products of TBP and n-dodecane (neutral). These are then susceptible to further degradation to neutral and acidic products.

The region before DBP (~5-12 min) represents degradation products of DBP, all acidic, such as MBP and other products such as MBP-$O(CH_2)_xCH_3$ which result from one of the butyl groups on DBP being fragmented, and phosphate which shows up in larger quantities especially during high LET irradiations which are more prone to secondary

degradation. Some of the peaks in the region between DBP and TBP (~12-15 min) represent DBP-$O(CH_2)_xCH_3$, neutral products of TBP where one of the butyl groups is fragmented. In fact, the peak for DBP represents both DBP that has been derivatized and DBP-OCH_3 resulting from TBP fragmentation (note the presence of a relatively smaller peak for DBP remains even when no derivatization agent is added, 11.6 min Figure 24).

The region between TBP and TPP (~15-23 min) represents neutral TBP and n-dodecane combination products (~19-23 min), the major ones being identified by GC-MS (Figure 25), and their respective acidic degradation products (15-19 min) which result from secondary or consecutive degradations. These come out before the combination products due to their decreased molecular weight and their acidity can be confirmed by observing their disappearance in the chromatogram of samples analyzed without diazomethane on the FPD (Figure 23 and Figure 24).

Neutral TBP and n-dodecane combination products (~19-23 min) were identified by mass spectrometry to be isomers of three main classes (Figure 25). These were condensation products of TBP and n-dodecane (MW = 434 gm/mol, a) Figure 25), TBP and n-dodecane where a butyl group on TBP is replaced by an n-dodecane molecule (MW = 378 gm/mol, b) Figure 25), and TBP and n-dodecane where an n-dodecane molecule replaces an oxybutyl on TBP resulting in a phosphonate bond (MW = 363 gm/mol, c) Figure 25).

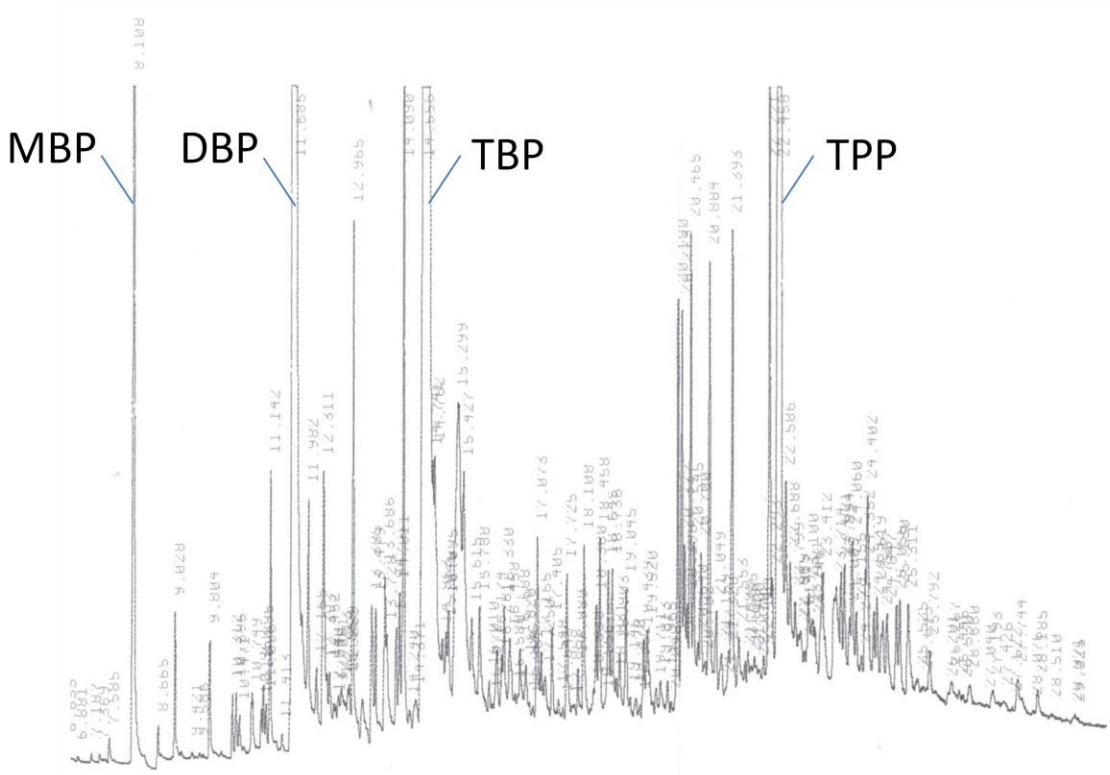

Figure 23. FPD analysis of 1M TBP post gamma irradiation. Note major peaks for MBP, DBP, TBP, and triphenyl phosphate. N-dodecane is absent since the FPD is sensitive to phosphorus containing compounds.

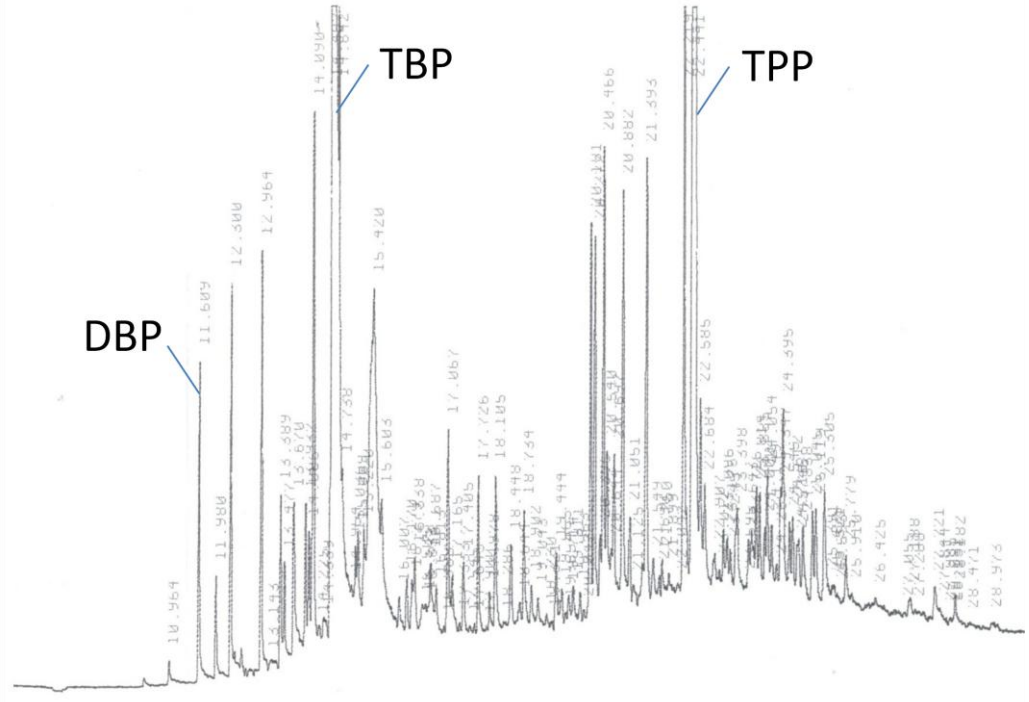

Figure 24. FPD analysis of 1M TBP post gamma irradiation without derivatization. Note major peaks absent for MBP, nearly absent for DBP, and present for TBP and triphenyl phosphate.

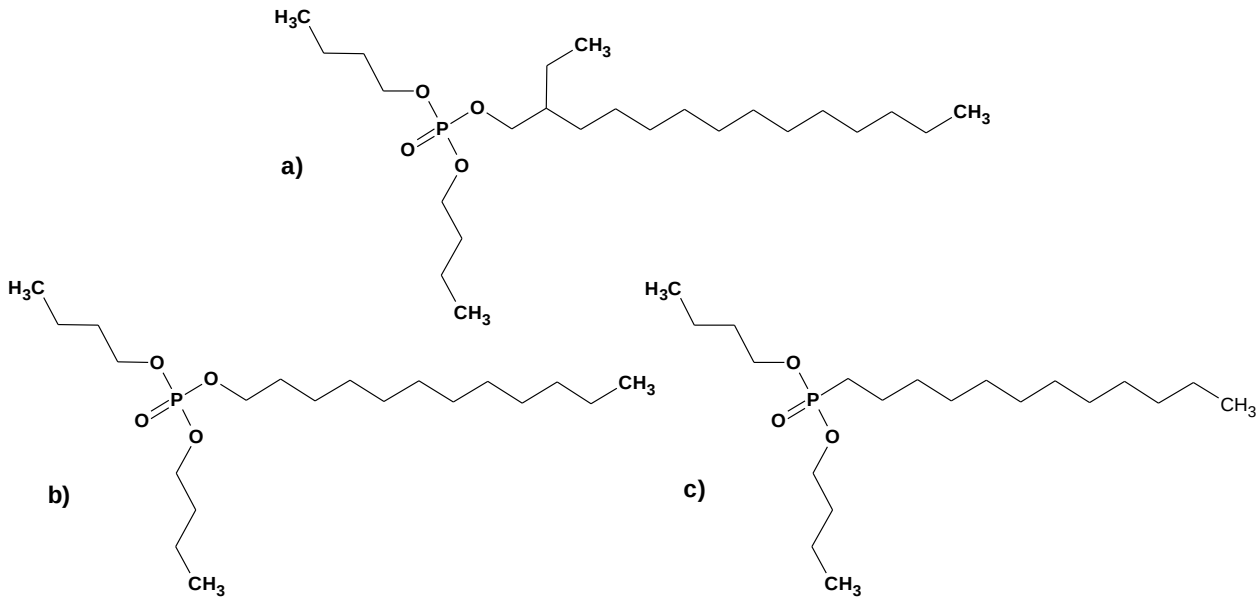

Figure 25. Potential condensation products of TBP and n-dodecane. Note that in contrast to Figure 3, structure is drawn out more completely to more easily visualize that bonds can be created between any of the 12 carbons of n-dodecane and the a) carbons, b) oxygen, or c) phosphorus on TBP resulting in a variety of isomers with the same molecular weight. In b) and c) a butyl and butoxy group are replaced respectively.

When derivatization agent diazomethane is not added, the acidic products do not appear in the chromatogram. These include DBP, acidic degradation products of DBP (~5-11.6 min, including MBP), and acidic degradation products of TBP/n-dodecane condensation products noted above (15-19 min). Some examples of peaks between 15-19 min that are not observed without derivatization agent are at 15.615, 15.788, 18.380, 18.645, 19.045, and 19.5 minutes. The peaks do not completely disappear, with a small portion remaining, but it is important to keep in mind that the peak in the chromatogram is the methylated version of the acid product. Therefore, as with DBP discussed above, for each of the high molecular weight products, there are resulting neutral fragmented products where only a methyl group remains which elute on the chromatogram at the same location as the derivatized acid product because they are identical molecules. It is also interesting to note that without addition of derivatization agent, the peaks between DBP

and TBP (12-15 min) and extra large molecular weight products (>23 minutes) remain. This is because these products are mainly neutral fragmentation products of TBP rather than acid products and neutral secondary polymer products of TBP/n-dodecane condensation products respectively.

Preliminary analysis summarizing all 100+ non TBP/DBP phosphorus containing (TBP derived) peak areas shows nearly a match with the difference between TBP and DBP peak area for both low and high LET irradiations. As it would be impractical to obtain standards and perform calibration curves for all of these products, a more manageable approach may be to determine an accurate method to estimate concentration from peak area based on attributes of the molecule and detection method. For example, for the FID, peak area can be correlated with molecular weight. Analysis of 1M TBP and 1M DBP revealed that peak area for 1M DBP was about 2/3 of the peak area for 1M TBP which about correlates to the difference in mass. In one instance it was observed that TBP was overlapping a molecule (product) with slightly higher molecular weight, perhaps by a single oxygen atom. The HP-624 column was able to separate this compound from TBP, however we were not able to identify it by MS since the GC equipped with the MS was unfortunately not equipped with this type of column.

On a strict comparison of peak area, it was possible to observe that for alpha and gamma irradiations where equivalent degradation of TBP was achieved, larger quantities of DBP and neutral high molecular weight condensation products were produced from gamma irradiation, and larger quantities of secondary products of DBP (MBP and phosphate) and neutral high molecular weight condensation products (high molecular weight acids and fragmented molecules) were observed for high LET radiation. We

attribute this to secondary degradation which occurs within the large width of the alpha track where reactive products are concentrated.

3.5 CMPO Irradiations

Solutions of 0.1 M CMPO in n-dodecane were irradiated in the gamma source receiving doses from 100 – 300 kGy. Solutions of 0.1 M CMPO in n-dodecane containing 0-0.15M bis(pinacolato)diboron were irradiated in the reactor at 250 kW for 2 hours receiving 100 – 350 kGy. Due to low solubility of bis(pinacolato)diboron in n-dodecane and a low concentration of the polar ligand CMPO, 0.15M was the maximum concentration that could be reached. This concentration was nevertheless sufficient to distinguish the effects of high LET radiation in the reactor and extract it from background low LET radiation in the reactor. Results are shown in Figure 26. Similar to previous irradiations, less degradation of CMPO was observed for high LET dose.

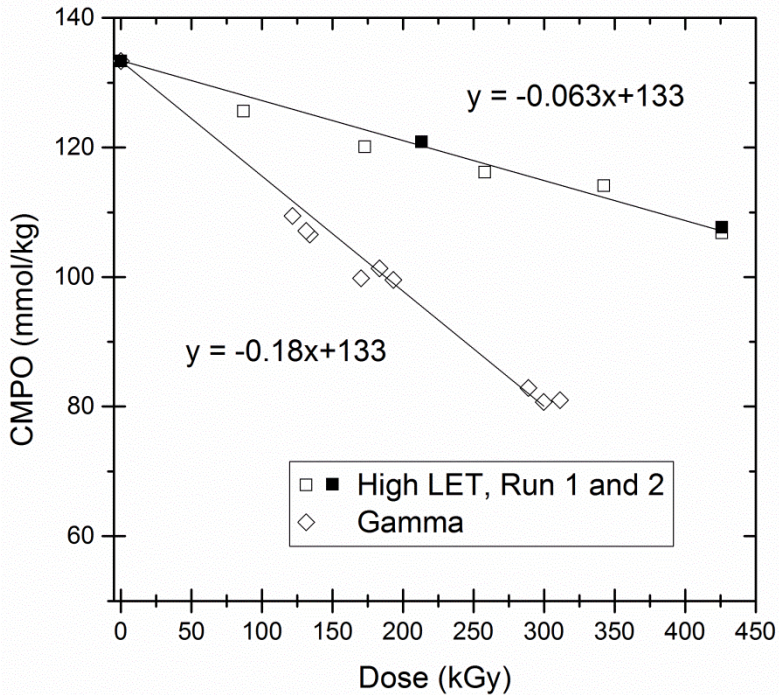

Figure 26. High and low LET radiolysis of 0.1M CMPO in n-dodecane. Slope reflects the G-value for degradation of CMPO and the values are given in this figure (-0.18 ± 0.01 μmol/J and -0.063 ± 0.006 μmol/J for low and high LET respectively).

CMPO degradation may have been suppressed when irradiated post contact with aqueous nitric acid compared to dry irradiations (Figure 27). Post irradiation extraction behavior was studied by performing americium-243 solvent extraction experiments on high LET irradiated solutions (Figure 28). Irradiation produces acidic products capable of extracting trivalent actinides (Mincher B. J. 2009). The formation of these products may be somewhat enhanced by the presence of nitric acid. Note that in Figure 28 there is a difference in extraction at the first set of points even though there is no alpha dose. This is because there was still background gamma dose in the reactor for samples containing no boron which created products that would elevate D values for americium-243.

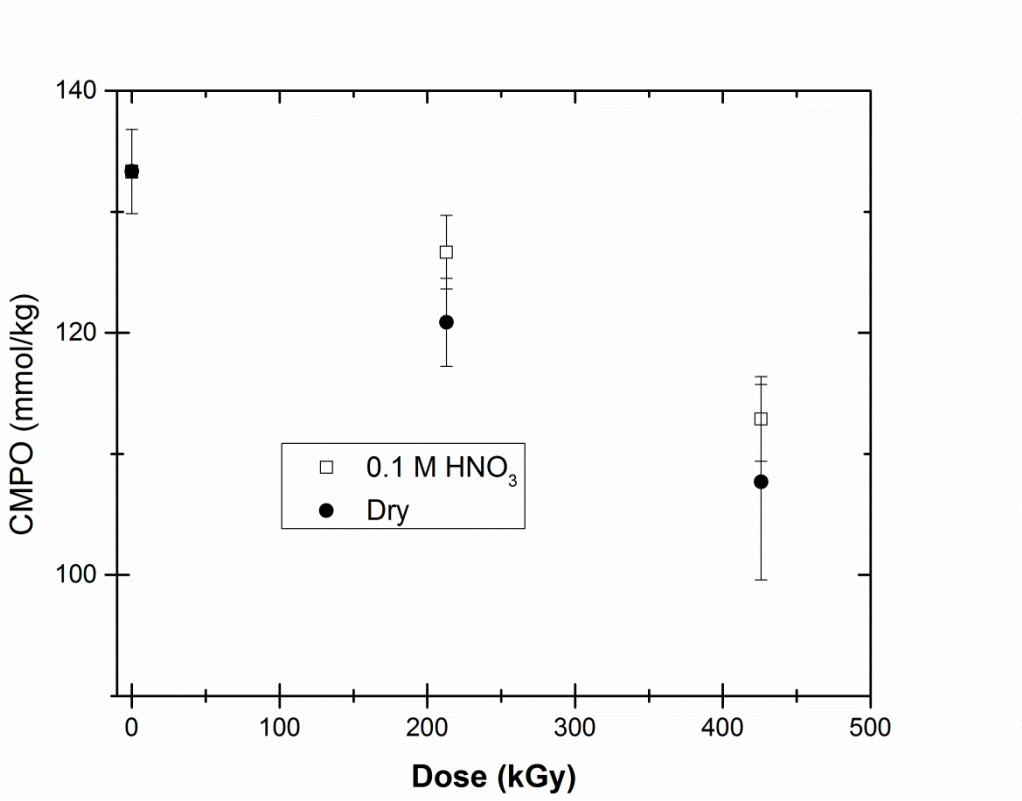

Figure 27. High LET irradiation of dry 0.1M CMPO/n-dodecane and post contact with 0.1M nitric acid. Error bars are from standard deviations calculated from triplicate samples.

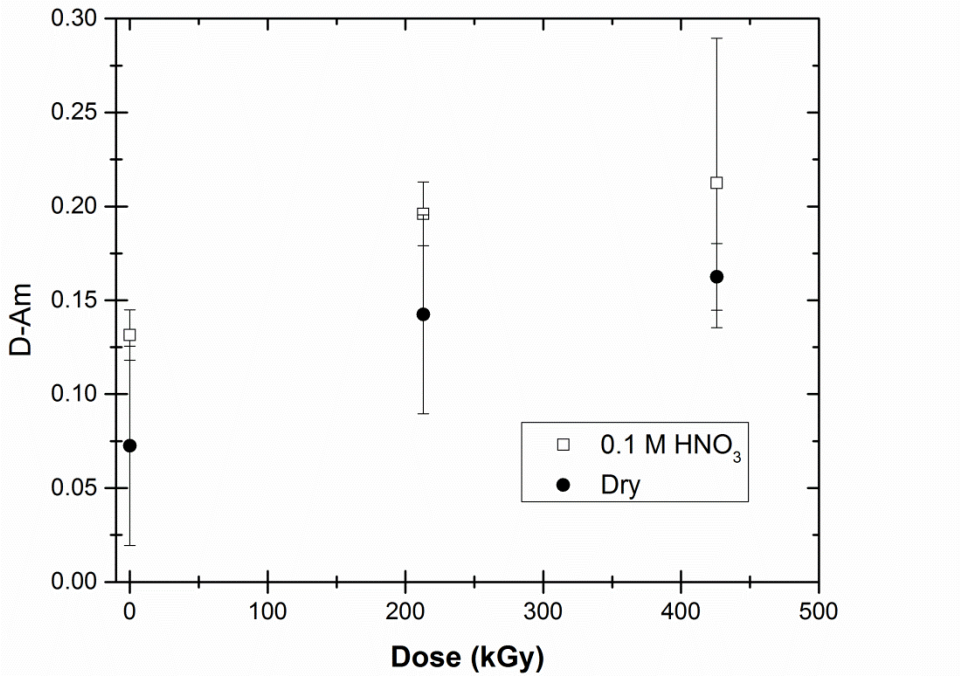

Figure 28. Dose dependence of measured americium distribution ratios for forward extraction of high LET irradiated solutions. Solutions were dry and pre-equilibrated with 0.1M HNO_3 prior to irradiation. Error bars are from standard deviations calculated from doublet samples.

Studies were also carried out with 3M HNO_3 contacted solutions, however HPLC analysis resulted in depressed levels of CMPO which at first were theorized to be due to some type of organic soluble nitric acid aggregation. NMR and chromatographic mass balance studies pointed to the possibility of CMPO leaving the organic phase (not entering the aqueous phase), and accumulating in a visually very difficult to discern third phase. Additional studies are necessary to determine conclusively the cause of this discrepancy at high acid concentration contacts.

3.6 TODGA Irradiations

0.1M solutions of TODGA in n-dodecane with 0-0.15M bis(pinacolato)diboron were irradiated in the reactor for 5 hours at 250 kW. 0.01M solutions of TODGA in n-dodecane with 0 – 0.125M bis(pinacolato)diboron were irradiated in the reactor for 1.5 hours at 250

kW. Two different concentrations were irradiated to observe the effect of concentration on degradation. Similar to the methylene blue studies, the background radiation from the reactor was utilized in the samples with 0M bis(pinacolato)diboron to determine low LET G(-)TODGA values. Results are shown in Table 4. As with the other ligands studied, degradation was less for high LET radiation compared to gamma. It is also apparent (as described in Figure 2) that G-values of degradation of TODGA are less at lower concentration because there is less TODGA available to degrade.

Table 4. G_{TODGA}^{-} values for low and high LET irradiated at 0.1M and 0.01M in n-dodecane.

	G(-)TODGA	
	Low LET	High LET
o.1 M TODGA	0.23 ± 0.05	0.08 ± 0.03
0.01M TODGA	0.083 ± 0.002	0.0104 ± 0.0003

4. DISCUSSION

As all types of high energy radiation, gamma (photons), beta (electrons), and alpha (ions) (with the exception of neutrons and high energy gammas and α-particles that can interact with the nucleus), essentially have the same physical effect of exciting/removing electrons and disrupting bonds of atoms within molecules. Any differences in product formation vs. dose from radiation types are dictated by the environment or track resulting from the unique respective LET of each radiation type considered to be the dominant physical parameter (LaVerne 2001). This is most clearly illustrated by work summarized for the Fricke dosimeter response to a variety of radiation LET types in Figure 6. Solution

conditions such as ligand concentration and presence of water, acid, and gases play a role as well in how profound an effect and what type of an effect track differences will have on the radiolysis process. Knowledge of these differences serves to anticipate the extent of degradation induced by specific types of radiation.

4.1 LET effects

4.1.1 Observed effects at same LET (high and low) and varying ligand concentration

One interesting revelation from our research was the widening gap between high and low LET effects observed as ligand concentrations of decreasing value are irradiated (Table 5). For dry systems, our results show that as ligand concentration decreases, G(-)Ligand decreases (Table 4 and Figure 2). However this decrease can occur to a lesser extent for low LET than high LET (Table 4) causing the increasing ratio seen in Table 5. As shown in the TODGA irradiations at different concentrations, a 10-fold decrease in the ligand concentration results in nearly a 7-fold drop in degradation by high LET but only a 3-fold drop in degradation induced by low LET. This phenomena can be described by radiation track chemistry and damage caused by reactive products within and outside of the tracks.

For low LET radiation ((Wilkinson 1961), Figure 2) a significant portion of radiolytic damage is caused by indirect radiolysis by reactive products produced from direct interaction with radiation which travel away from their site of origin and preferentially are attracted to and degrade the polar parent ligands. Low LET radiolysis can be dominated by this type of mechanism.

As LET increases towards high LET radiation, in which reactive products are confined densely in a much smaller volume, primary reactive products have increased

probability of participating in indirect secondary reactions with ligand degradation products or with themselves rather than parent ligands. This is both due to the increased presence of these species and due to the decreased presence or consumption of parent ligand within the track. This can be visualized with a theoretical figure for what high LET response may look like if plotted against ligand concentration (Figure 29). For high LET, radiation as reactive products react less with the parent ligand and more with degradation products and with themselves. This decreases parent ligand degradation in a neat scenario (volume fraction of ligand = 1) for gamma compared to high LET. It is shown in Figure 29 as a lower G-Acid at x = 1 compared to low LET. High LET could give the appearance of adhering to the mixture law better for volume fractions between 0 and 1. Points in Table 4 could be the first points to a figure similar to Figure 29 (do a search for or irradiate pure TODGA, and prepare figure 29 with those actual points from Table 4). In-between the volume fraction of 0 and 1 as low LET response tapers off to near slope = 0, there is a region where decrease in degradation rate vs. decrease in ligand concentration has a higher slope for high LET vs. Low LET.

Table 5. Difference in response between low and high LET increases as ligand concentration decreases.

Compound/Concentration	Low LET/High LET yield
1M TBP	2.6
0.1M CMPO	3
0.1M TODGA	3
0.01M TODGA	8
18 μM Methyl Red	15
16 μM Methylene Blue	24

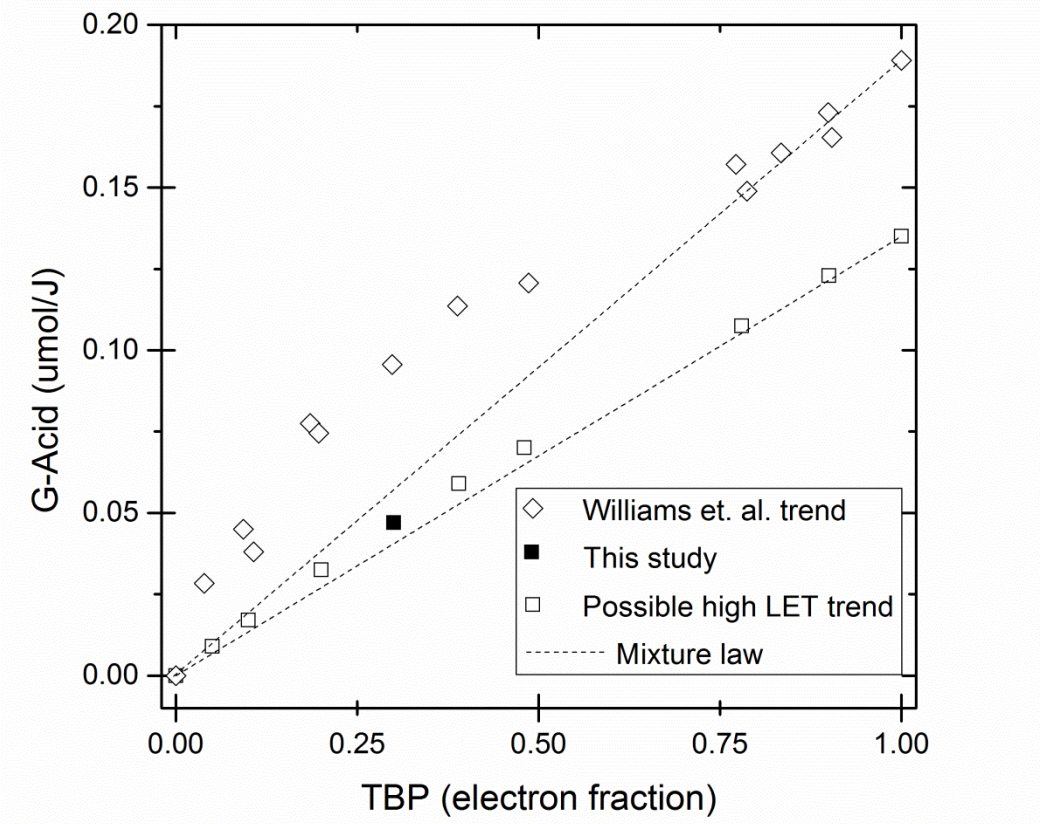

Figure 29. Hypothetical scenario of low LET (diamond) vs. high LET (square) response at different ligand concentrations. Initial direct degradation from radiation does not discriminate between ligand or diluents. It is the secondary reactions, the extent to which reactive products can reach parent ligand that deviation from the mixture law occurs. This deviation may occur to a lesser extent for high LET radiation where parent ligand is degraded within the tracks and both other reactive products and degraded ligand compete to absorb reactive products.

4.1.2 Holding ligand concentration constant and varying LET

The effect of LET has special importance, especially when considering the degradation of ligands utilized in used nuclear fuel separation applications, because used nuclear fuel contains both high and low LET radiation emitters. Levels of individual radiation emitters can vary from one process step and ligand to the next, as isotopes are extracted. Additionally, for used nuclear fuel, high LET emitting elements emit ~5.5 MeV helium ions (LET = ~90 eV/nm) and our method studies the effects of 1.5 MeV helium and 0.8 MeV lithium ions (LET slightly above 200 eV/nm). With sufficient data similar to Figure 6, an

adjustment can be made based on data obtained experimentally to determine the effect of 5.5 MeV alphas.

Figure 30 presents our most thorough attempt at achieving such a plot for DBP formation during radiolysis of dry 1M TBP/n-dodecane solutions. This figure contains DBP formations from our results for low LET gamma radiation (^{137}Cs) and the high LET $^{10}B(n,\alpha)^{7}Li$ reaction at the far left and right respectively. The other two points are DBP formation from irradiation with 10.4 MeV helium ions from an ion beam (Ladrielle 1983) and predicted DBP formation from 5.5 MeV alphas from plutonium (Kawaguchi 2009). The observer can see that there appears to be a near linear trend for DBP based on LET similar to that for the Fricke system. We could estimate a similar linear correction to better compare our results found for methylene blue, DBP, TODGA at high LET to others reported in the literature (See Figure 31 for methylene blue).

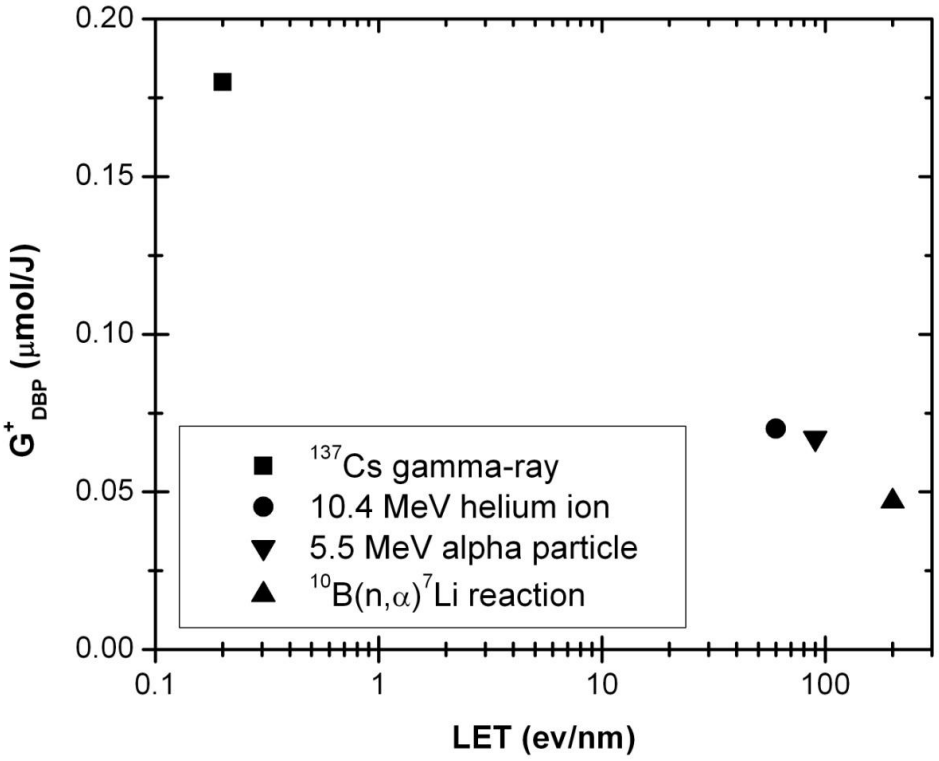

Figure 30. Correlation of LET and formation of DBP during irradiation of 1M TBP in n-dodecane. Data for gamma ray and $^{10}B(n,\alpha)^{7}Li$ reaction is taken from this work. The data for the 10.4 MeV and 5.5 MeV alpha particles are taken from Ladrielle et al.(Ladrielle 1983) and Kawaguchi et al.,(Kawaguchi 2009) respectively. Data reproduced from Pearson and Nilsson (Pearson 2014) with permission from Taylor and Francis.

4.2 Comparison to G-values reported in the literature

With the proper adjustment for LET our results can be compared to results in the literature for the ligands we studied for low and high LET (Table 6). There is good agreement which supports using the $^{10}B(n,\alpha)^{7}Li$ reaction as an alternative method for studying high LET radiation. An adjustment to the value obtained for the $^{10}B(n,\alpha)^{7}Li$ reaction, up to a G(-) methylene blue of 0.15 μmol/J for a 10 MeV alpha, brackets the value reported by LaVerne et al. for helium ions of similar LET (LaVerne 2005)(Figure 31). While LaVerne did report a difference in G(-)methylene blue for protons of different LET he did not observe a change for helium ions with different LET (Figure 31). This is not unreasonable considering that a

flattening is observed in the G-values as very high LET is approached in the Fricke dosimeter (Figure 6,(Allen 1961)). However, their data for 2 MeV did not extend up to the dose range of this study and a dependence on LET could also potentially be within error of the experiment. In either case what is important to consider is that with adjustment for LET, our values for high LET are within the same range of those reported by LaVerne (LaVerne 2005).

Table 6. G-values (μmol/J) of various ligands and degradation products investigated in this study compared to those found in the literature for both gamma and alpha radiation

Ligand/degradation product	Literature	This study
G(-)methylene blue (16 μM) Gamma	0.074 (LaVerne 2005) ± 0.004	0.070 ± 0.008
G(-)methylene blue (16 μM) Alpha	0.007 (LaVerne 2005)** ± 0.003	0.003 – 0.015***
G-DBP (1M TBP) Gamma	0.17 average of two studies: (Burger 1958, Egorov 2005)	0.18 ± 0.01
G-DBP (1M TBP) Alpha	0.067 (Kawaguchi 2009) ± N/A	0.063* ± 0.002
G(-)TODGA (0.01M/L TODGA) Gamma	0.080 (Sugo 2009) ± 0.003	0.083 ± 0.002
G(-)TODGA (0.01M/L TODGA) Alpha	0.022 (Sugo 2009) ± 0.001	0.020* ± 0.001

*Estimated for 5.5 MeV alpha based on LET
**Value reported for 2, 5, and 10 MeV helium ions, no difference was observed by authors
***No adjustment (0.003) and adjustment to 10 MeV helium ion (0.015)

Surprisingly, possibly due to the lack of sophisticated GC techniques in the past as well as the focus on DBP, there is little to no data in the literature on values for G(-)TBP much of which consist of summations of degradation products that are equated to TBP loss

(Adamov 1990). This is a very interesting comparison which is not included in Table 6. Any future studies at varying conditions which concurrently monitor TBP as well as DBP, will make an immediate contribution to the literature and likely yield new insights to the degradation characteristics.

Additional data for alpha radiolysis of CMPO is currently being collected by collaborators at Idaho National Lab and Cal State University Long Beach. Current data collected at these institutions did not observe a response to alpha radiation possibly due to doses which were not high enough to resolve trend. Therefore data from the literature is not included in Table 6 for comparison for CMPO.

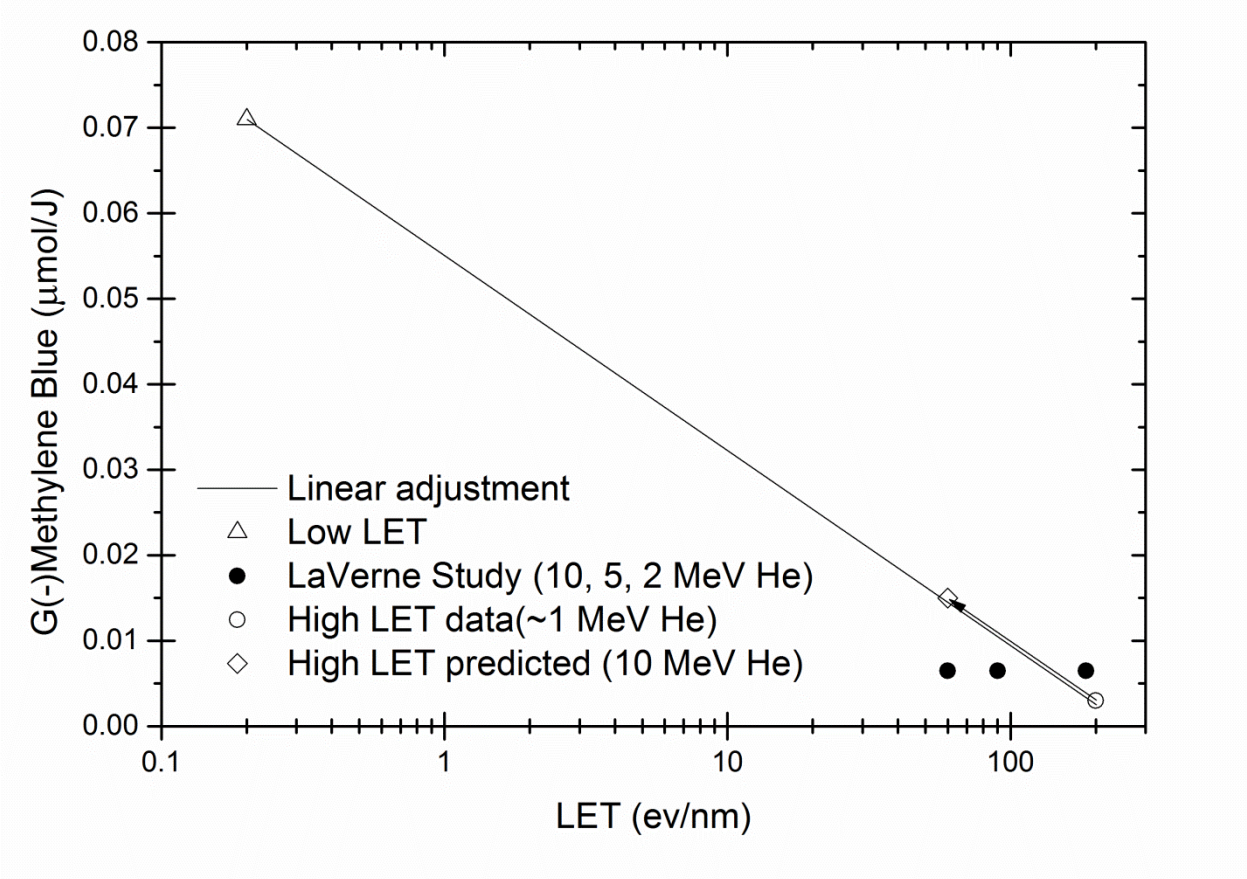

Figure 31. Correlation of LET and degradation of methlyene blue. Demonstrates the linear adjustment to predict the effect of a 10 MeV alpha particle with an LET of 60 eV/nm and compares those to the G-value found by LaVerne by helium ions of energies 2, 5, and 10 MeV.

4.3 Effect of water, nitric acid, and metal ion contact

A discussion of the effects of water and nitric acid contact is best approached by viewing trends in our data and in the literature for TBP radiolysis since it is the compound most thoroughly studied. These findings are shown in Table 7 and Table 8 for low and high LET radiolysis respectively of TBP.

Table 7. Selected G^{+}_{DBP} values for gamma irradiated TBP/alkane solutions.

Source	Author(s)	Solution	Irradiation Conditions	G^{+}_{DBP} (µmol/J)
^{60}Co	(Burger 1958)	30% TBP/isooctane	No pretreatment, 'dry'	0.19[a]
^{137}Cs	(This study)	1M TBP/n-dodecane	No pretreatment, 'dry'	0.18
^{60}Co	(Egorov 2005)	30% TBP/decane	No pretreatment, 'dry'	0.15
^{90}Sr	(Becker 1983)	30% TBP/alkane	In contact with 3M HNO_3	0.11
^{60}Co	(Hui-bo 2012)	30% TBP/kerosene	Pre-equilibrated with 3M HNO_3	0.10
Low LET	(Schulz 1984) (Graphic interpolation of various studies)	30% TBP in Aliphatic Diluents	H_2O Saturated	0.09

[a]Values represent G-mono-acid-phosphates rather than DBP specifically

Table 8. Selected G^{+}_{DBP} values for alpha irradiated TBP/alkane solutions

Source	Author(s)	Solution	Irradiation Conditions	G^{+}_{DBP} (µmol/J)
Helium ion beam	(Ladrielle 1983)	30% TBP/n-dodecane	Sealed in quartz "Dry"	0.07[b]
$^{10}B(n,\alpha)^{7}Li$ reaction	(This study)	1M TBP/n-dodecane	Sealed in polyvials "Dry"	0.063
Pu^{238}	(Hui-bo 2012)	30% TBP/ kerosene	Pre-equilibrated with 3M HNO_3	0.08[c]
Pu^{238}	(Kawaguchi 2009)	30%TBP/n-dodecane	Pre-equilibrated with 3M HNO_3	0.09[c] (0.067)[d]
Pu^{238}	(Lloyd 1985)	30% TBP/n-dodecane	Pre-equilibrated with 3M HNO_3	0.10[c]
Pu^{238}	(Kulikov 1983)	30% TBP/paraffin	In contact with 3M HNO_3	0.10[c]

[b]Estimated from extrapolation in figure. Helium ion tuned to 10.4 MeV for irradiation.
[c]The DPB formation represents total formation from degradation of TBP from radiolysis, acid hydrolysis, and metal ion catalyzed hydrolysis.
[d]Kawaguchi predicted a G-DBP of 0.067 µmol/J, for radiolysis effects alone to the system after removing acid and metal effects.

These two tables show evidence that aqueous nitric acid contact prior to irradiation reduces DBP formation for gamma radiation (which is well described for aqueous contact (Schulz 1984)), while the reverse occurs for high LET irradiation. A potential explanation may be the presence of metal ions. Lloyd and Fellows (Lloyd 1985) concluded in their studies that metal ion catalyzed hydrolysis can potentially be a contributor to half of the DBP formation. Furthermore, Pu irradiations can last days, 7-80 days for Lloyd and Fellows. For exposures lasting several days, acid hydrolysis becomes more relevant to DBP formation relative to radiation-induced formation. Additionally, the large circumference of an alpha may potentially allow elevations in temperature which could increase DBP

formation for alpha radiation when nitric acid is present, more so potentially than it does for gamma radiation. Removing these contributions to reflect radiolysis effects only for and aqueous contacted system exposed to alpha radiation, would reduce the reported values for DBP formation from ^{238}Pu in Table 8 to levels below those reported for dry systems, mirroring the aqueous protection effect trends seen for gamma radiolysis.

The effect of reducing DBP formation from adding aqueous solutions is interesting. Both water and nitric acid complexes with TBP have been described as potentially having a protective effect on TBP (Mincher B. J. 2009). However reduced DBP formation does not necessarily imply (without concurrently monitoring TBP levels to confirm) that TBP degradation also decreased as it may have degraded through an alternate pathway. It may be more proper to say that significant research has shown that dissolved water reduces acid yields (DBP) in the gamma radiolysis of TBP (Schulz 1984). This is why it is critical to concurrently monitor TBP and other degradation products to obtain a complete picture of the degradation process. Utilizing our method without the presence of metal ions can also potentially shed additional light on what degradation reactions are happening and what the causes are.

4.4 Significance of the presence of many types of degradation products

Equipped with an understanding of the reaction mechanisms and their causes, we can more effectively track and potentially avoid the formation of the so-called ligands that have a detrimental effect on solvent extraction processes to improve process performance and efficiency. While our data on dry systems shows dramatic decrease in degradation for all ligands studied for high LET vs. low LET radiation, this does not necessarily mean that

alpha radiation is more benign towards a solvent extraction process than low LET radiation. Alpha radiation is often considered to have nearly equal to worse effects (Kulikov 1981, Ladrielle 1983, Hui-bo 2012). What we have described above is the importance of taking metal ion catalyzed reactions and track conditions into account when making such comparisons. But more important is the formation of secondary products within the alpha track. These are the products high molecular weight, such as dialkyl acids and hydroxamic acids (Figure 3), that cannot be removed with a sodium carbonate scrub as is a general practice in the PUREX process. Hui bo attributes worse extraction performance of irradiated TBP solutions to the presence of these secondary products (Hui-bo 2012).

In CMPO studies shown in Figures 26 – 28, alpha radiolysis for the dry system destroys less of the parent compound than gamma radiolysis. Although we did not concurrently monitor the formation of degradation products for a comparison of high LET to gamma, we did perform solvent extraction experiments which are a reflection of these degradation products. Similar to studies by Mezyk (Mezyk 2013) for gamma radiolysis, degradation products appeared which enhanced the extraction of ^{243}Am, notwithstanding the 15-20% loss in CMPO extractant. Based on ^{243}Am distribution ratios, formation of these products appears more drastic per dose for gamma radiation. For instance, Mincher et al. found D Am increases from 0.15 up to 0.35 after 400 kGy for gamma, while in our study D Am increased to about 0.20 after 400 kGy of high LET (including ~80 kGy gamma background). However whether or not these products differ for high LET vs. gamma, have differing resistances to stripping, or are more or less are difficult to remove in a wash for high LET vs. gamma is still unknown. Decrease in selectivity is also unknown which is an important factor for determining how detrimental these products are to the process.

Contact with an aqueous nitric acid phase prior to high LET radiolysis appears to also reduce the degradation of CMPO while it appears to increase the ^{243}Am distribution ratios suggesting that the acid may promote formation of more detrimental products while at the same time protecting CMPO. This may suggest evidence of the presence of hydroxamic acids resulting from nitric acid nitration reactions. However this increase in ^{243}Am distribution ratios was observed for both high LET and gamma dose (0M Boron concentration) which conflicts with findings that 0.1M nitric acid presence reduces ^{243}Am distribution ratios for 0.1M CMPO systems exposed to low LET radiation (Mezyk 2013). Therefore it is difficult at this time to draw conclusions on the differences between alpha and gamma and dry and acid conditions for CMPO.

4.5 Selecting the most optimal ligand and process conditions for a used fuel solvent extraction process with regards to radiolysis

Numerous solvent extraction ligands must be vetted prior to large and expensive pilot scale demonstrations. Response to radiation must be factored in while determining which ligands are the most optimal for use.

A first step in examining the response to radiation is to determine what type of radiation is more prevalent in the process step of interest (i.e. what radioisotopes will be present and in which phase, organic or aqueous) and then use the appropriate radiation source for radiolysis studies.

If excess ligand is not necessary, reduced concentrations may be considered which decrease the formation of degradation products per dose, most especially for alpha, against

which molecules in this study have demonstrated accelerated resistance as concentration decreases.

Another important factor is to determine how bad the degradation products are. More concern should be given to degradation products that will negatively impact the process vs. others whose effects will be benign.

Taking into consideration all of these factors, one may determine which molecules overall have the most attractive resistances and responses to radiolysis. In our work we made an attempt to compare the performance of 0.1M CMPO to 0.1M TODGA in n-dodecane which are both under consideration for a TRUEX type process. Our results showed similar resistance to alpha radiation for both compounds, and perhaps a slightly greater resistance to gamma radiation for CMPO, but within error these responses are potentially very similar as well. Our results, along with others (Groenewold 2012, Mezyk 2013, Mincher 2014), show that radiolysis of CMPO forms acidic products that enhance ^{243}Am extraction but may not impede it from being stripped. In alpha radiolysis studies on the TRUEX process some negative plutonium retention characteristics were observed, but this may have been the result of TBP degradation products as TBP is also part of the TRUEX solvent (Bushholz 1996). Whether or not similar undesirable products are formed from TODGA was not studied. While TODGA shows similar resistance to radiation, it could be selected as superior on the merits of not forming as many detrimental products that interrupt extraction were this attribute observed and confirmed.

5. CONCLUSIONS

Radiolysis is detrimental to solvent extraction processes developed for used nuclear fuel separations, contributing to loss in ligand, loss in selectivity due to degradation products, and losses in solvent quality due to formation of surfactants and high molecular weight compounds.

LET is shown to have a large impact on radiolysis to used nuclear fuel solvent extraction processes, controlling the extent to which degradation occurs as well as the process conditions and chemistry that determines which of a variety of degradation pathways and products are followed.

Utilizing the $^{10}B(n,\alpha)^{7}Li$ reaction is an attractive alternative to helium ion and radioactive isotope high LET radiolysis methods due to its ability to rapidly achieve high doses without contaminating a sample with radioactive metals, as well as study high LET effects apart from metal ion catalyzed hydrolysis.

Research demonstrates that studying the effects of high LET radiation based on the $^{10}B(n,\alpha)^{7}Li$ reaction in a mixed radiation field in a reactor is not an insurmountable challenge and can yield excellent results. Both gamma and high LET radiolysis responses for methylene blue, TBP, and TODGA compare well with those found in the literature. If desired, it appears possible to make an LET adjustment to the $^{10}B(n,\alpha)^{7}Li$ reaction response to estimate the response of a 5 MeV alpha particle.

Degradation and product formation decreases as ligand concentration decreases and at some concentrations can do so more rapidly for alpha than gamma. High LET induced degradation to a ligand is typically less than that of low LET for dry systems due to isolation of reactive products in the radiation track, however this isolation tends to enhance the formation of secondary products which tend to be acids possessing undesirable extraction characteristics.

To obtain a more complete picture of radiolysis it is critical to monitor the parent ligand concentration in tandem with the degradation products at a variety of process conditions such as dry, water contacted, and acid contacted and for different types of radiation to account for the wide diversity of products that can be formed.

6. FUTURE WORK

It is desirable to do more extensive and quantitative water and acid contact studies on solvent extraction compounds, especially TBP. In addition to monitoring TBP concentrations, degradation products can be monitored and quantified to create a complete mass balance and enhanced picture of the reactions that occur across multiple process conditions, in addition to high and low LET.

There is some debate in the literature on whether the plutonium retaining degradation products formed during TBP radiolysis that cannot be removed by alkaline washes are mainly alkyl phosphoric acids formed in secondary reactions or hydroxamic acids formed in secondary reactions to hydrocarbon nitration. We have the capacity in our

laboratory to examine this, and may find benefit in using the nitrogen-phosphorus detector on the GC, post acid contact studies, to observe nitrated compounds and hydroxamic acids.

The ability to perform organic and aqueous mixed phase radiolysis studies is being developed in the lab for both the ^{137}Cs gamma cell and the reactor. A mixing system and pumped closed loop are nearly complete for both. Alpha radiolysis studies add an additional layer of complexity to two phase gamma radiolysis studies in that alpha particles deposit their energy in the phase in which they are found due to their short distances travelled. In a solvent extraction process, alpha particles from alpha emitting isotopes confined mainly to the aqueous phase may never reach the organic phase where the ligands are present. In contrast alpha emitting particles in the organic phase will damage extraction ligands. There is a unique opportunity here with organic soluble boron compounds and aqueous soluble boric acid to study high LET radiation in the precise organic/aqueous distributions encountered in a particular solvent extraction process of interest. Furthermore, a mixed loop system will take into account alpha energy lost as it passes into the aqueous phase (Figure 32). With 10-boron activation, all of these scenarios will allow for an examination of high LET effects without the presence of metal ion catalyzed hydrolysis effects. This method also has the ability to take advantage of background radiation in the reactor to study the effects of mixed radiation fields, to further verify whether or not there is any interaction, and observe any interaction that may appear as dose rates increase beyond those present in our current studies.

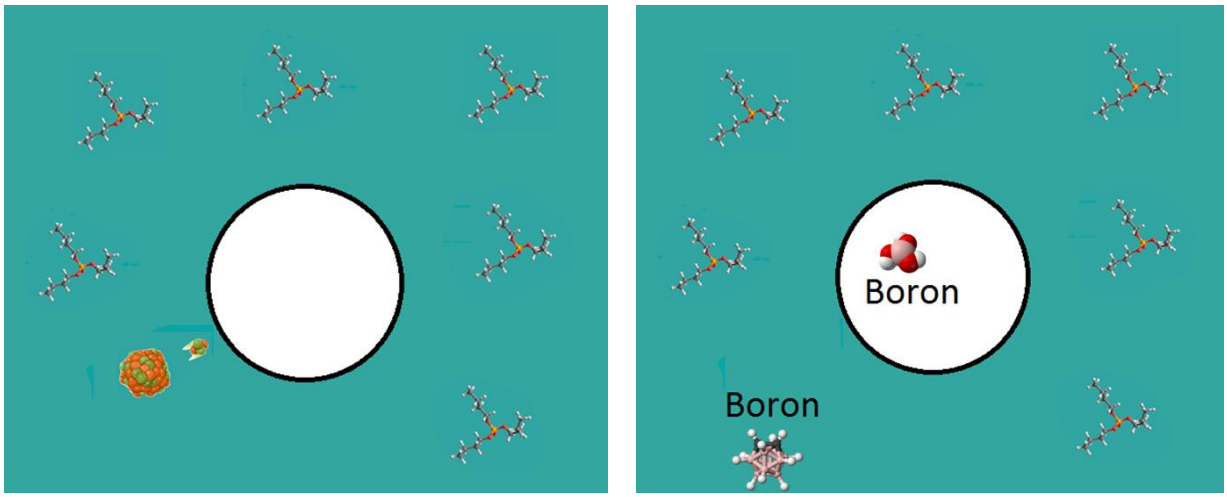

Figure 32. Two phase radiolysis studies. Alpha particles will lose energy if they are within or pass through the aqueous phase. Organic and aqueous soluble 10-boron sources such as carborane and boric acid can be used to create the precise alpha emitting isotope distributions encountered in a solvent extraction process.

The exponential equations derived in this study to describe the degradation of TBP assume an even stirred tank distribution of reactive products, parent ligand, and degradation intermediates. In reality, this is not the case. Reactive products are confined near radiation tracks, especially for high LET radiation, where parent ligand can be consumed to levels less than the average in the surroundings and degradation products can increase to high concentrations in excess of the surroundings, before all molecules and reactive products are evenly dispersed throughout the solution. This elevates observed overall rates of secondary reactions. More sophisticated models which take into account these track differences and track chemistry can be developed to more accurately model and describe the degradation occurring. Perhaps unique insight may be derived from developing and contributing to models which describe degradation in just a high LET track itself rather than the solution as a whole, as has been done in some studies (Green 1990, Science 1998).

References

Adamov, V. M., Andreev, V. I., Belyaev, B. N., Markov, G. S., Polyakov, M. S., Ritari, A. E., Shil'nikov, A. Y. (1990). "Identification of decomposition products of extraction systems based on tri-n-butyl phosphate in aliphatic hydrocarbons." Kerntechnik **55**: 133-137.

Allen, A. O. (1961). The Radiation Chemistry of Water and Aqueous Solutions, D. van Nostrand.

Becker, R., Stieglitz, L., Bautz, H. (1983). Radiolytic TBP degradation under PUREX process conditions. KfK 3639, PWA 66/83, Karlsruhe: Kernforschungszentrum, Karlsruhe, Germany. Karlsruhe, Germany 221-265.

Broshkevich, R., Kozlovska-Mil'ner, E., Novak, Z. (1973). "Radiolysis of the system HNO3-TBP." Radiokhimiya **15**: 280-282.

Burger, L. L., McClanahan, E. D. (1958). "Tributyl phosphate and its dilutent systems." Ind Eng Chem **50**(2): 153-156.

Bushholz, B. A., Nunez, L., Vandergrift, G. G. (1996). "Effect of α-Radiolysis on TRUEX-NPH Solvent." Separation Science and Technology **31**(16): 2231-2243.

Choppin, G., Liljenzin, J., Rydberg, J. (2002). Radiochemistry and Nuclear Chemistry. Woburn, MA, Butterworth-Heinemann.

Cohen, B. L. (1983). "Breeder reactors: A renewable energy source." Am. J. Phys. **51**(1): 75-76.

Crofoot, T. A. (1989). The determination of oxygen isotopic concentrations by neutron activation analysis and application to the determination of oxygen functional groups in coal by isotopic exchange. Department of Chemistry. University of California Irvine, University of California Irvine.

Egorov, G. F., Tkhorzhnitskii, G. P., Zilberman, B.Y., Shmidt, O. V., Goletskii, N. D. (2005). "Radiation chemical behavior of tributyl phosphate, dibutyl phosphoric acid, and its zirconium salt in organic solutions and two phase systems." Radiochemistry **47**(4): 392-397.

Fermvik, A. (2011). Radiolytic degradation of BTBP type molecules for treatment of used nuclear fuel by solvent extraction. Department of Chemical and Biological Engineering. Gothernburg, Sweeden, Chalmers University of Technology.

Gatrone, R. C., Rickert, P. G., Howritz, E. P. (1990). "Analysis of n-octyl(phenyl)-N,Ndiisobutylcarbamoyhnethylphosphine oxide and TRUEX process solvent by gas and liquid chromatography." Journal of Chromatography **516**(395-404).

Gelis, A. V., Lumetta, G. J. (2014). "Actinide Lanthanide Separation Process-ALSEP " Industrial & Engineering Chemistry Research **53**(4): 1624-1631.

GeneralAtomic (1969). TRIGA MARK I 250 KW Pulsing Reactor Mechanical Maintenance and Operating Manual.

Genter, W., Maier-Leibnitz, H., Bothe, W. (1954). An Atlas of Typical Expansion Chamber Photographs. London, Pergamon Press.

Green, N. J. B., Pilling, M. J., Pimblott, S. M., Clifford, P. (1990). "Stochastic Modeling of Fast Kinetics in a Radiation Track." J Phys Chem **94**: 251-258.

Groenewold, G. S., Elias, G., Mincher, B. J., Mezyk, S. P., LaVerne J. A. (2012). "Characterization of CMPO and its radiolysis products by direct infusion ESI-MS." Talanta **99**: 909-917.

Hawthorne, M. R. (1998). "New horizons for therapy based on the boron neutron capture reaction." Mol Med Today **4**(174-181).

Healy, T. V. (1976). "Fuel Reprocessing Solvent Tributyl Phosphate." Management of radioactive wastes from the nuclear fuel cycle: proceedings of a syposium on the management of radioactive wastes from the nuclear fuel cycle **1, STI/PUB/433, IAEA-SM-207-23(**Proceedings series: STI/PUB/43): 201-214.

Holland, J. P., Merklin, J. F., Razvi, J. (1978). "The radiolysis of dodecane-tributyl phosphate solutions." Nucl. Instrum. Methods **153**(2-3): 589-593.

Hui-bo, L., Zhe, S., Hai-feng, C., Feng-li, S., Xiao-rong, W., Hui, H., Zhan-yuan, L., Can-sheng, L. (2012). "α and γ irradiation stability of 30% TBP-kerosene-HNO3 systems." Journal of Nuclear and Radiochemistry **34**(5): 281–285.

Inoue, T., Koch, L. (2008). "Development of pyroprocessing and its future direction." Nuclear Engineering and Technology **40**(3): 183-190.

Kawaguchi, Y., Morimoto, K., Kitao, T., Ohyama, K., Omori, E. (2009). "Study of solvent degradation in reprocessing MOX spent fuel solvent degradation and its effects on Pu purification cycle." Trans. Atomic Energy Soc. Japan **8**(3): 221-229.

Kulikov, I. A., Kermanova, N. V., Sosnovskii, O. A., Shesterikov, N. N., Vladimirova, M. V. (1981). "Effect of alpha- and gamma- radiations on the decomposition of tributyl phosphate and the distribution coefficients of Pu4+ and Zr4+." Radiokhimiya **23**(6): 825-831.

Kulikov, I. A., Kermanova, N. V., Vladimirova, M. V (1983). "Radiolysis of TBP in the presence of plutonium and uranium." Sov. Radiochem. **25**: 310-316.

Ladrielle, T., Wanet, P., Lemaire, D., Apers, D. J. (1983). "Alpha and Gamma induced radiolysis of tributyl phosphate." Radioanal Lett **59**(5-6): 355-363.

Lamarsh, J. R. (2002). Introduction to Nuclear Reactor Theory. LaGrange Park, IL, American Nuclear Society, Inc.

LaVerne, J. A., Chang Z., Araos M. S. (2001). "Heavy ion radiolysis of organic materials." Radiat. Phys. Chem. **60**: 253-257.

LaVerne, J. A., Tandon, L., Knippel, B. C., Montoya, V. M. (2005). "Heavy ion radiolysis of methylene blue." Radiat. Phys. Chem. **72**: 143-147.

Lloyd, M. H., Fellows, R.L. (1985). Alpha Radiolysis and other factors affecting hydrolysis of trybutyl phosphate.

Madic, C., Hudson, M. J., Liljenzin, J-O., Glatz, J-P., Nannicini, R., Facchini, A., Kolarik, Z., Odoj, R. (2002). "Recent Achievements in the Development of Partitioning Processes of Minor Actinides From Nuclear Wastes Obtained in the Frame of the NEWPART European Programme (1996-1999)." Prog. Nucl. Energ. **40**(3 4): 523-526.

Mathur, J. N., Murali, M. S., Nash, K. L. (2001). "Actinide partitioning-a review." Solvent Extr. Ion Exch. **19**(3): 357-390.

Mezyk, S. P., Mincher, B. J., Ekberg, C., Skarnemark, G. (2013). "Alpha and gamma radiolysis of nuclear solvent extraction ligands used for An(III) and Ln(III) separations." J Radioanal Nucl Chem **296**(2): 711-715.

Miller, G. E. (2012). Radiation levels in reactor. J. Pearson. email.

Mincher B. J., M. G., Mezyk S. P. (2009). "Review article: The effects of radiation chemistry on solvent extraction: 1. Conditions in acidic solution and a review of TBP radiolysis." Solvent Extr. Ion Exch. **27**(2): 1-25.

Mincher, B. J., Mezyk, S. P., Elias, G., Groenewold, G. S., Ekberg, C., Skarnemark, G., LaVerne, J. A., Nilsson, M., Pearson, J., Schmitt, N. C., Tillotson, R. D. (2014). "The radiation chemistry of CMPO: Part 2. Alpha Radiolysis." J Solvent Extraction and Ion Exchange **32**(2): 167-178

MIT. "22.55 “Principles of Radiation Interactions” Radiation Interactions: neutrons." Retrieved 8/22, 2014, from http://ocw.mit.edu/courses/nuclear-engineering/22-55j-principles-of-radiation-interactions-fall-2004/lecture-notes/ener_depo_neutro.pdf.

Pearson, J., Jan, O., Miller, G. E., Nilsson, M. (2012). "Studies of high linear energy transfer dosimetry by 10B(n,a)7Li reactions in aqueous and organic solvents." J Radioanal Nucl Chem **292**: 719–727.

Pearson, J., Nilsson, M. (2014). "Radiolysis of Tributyl Phosphate by Particles of High Linear Energy Transfer." Solvent Extraction and Ion Exchange **32**: 584-600.

Pearson J., J. O., Wariner A., Miller G. E., Nilsson M. (2013). "Development of a method for high LET irradiation of liquid systems." J. Radioanal. Nucl. Chem. **298**(2): 1401-1409.

Pleasonton, F., Ferguson, R., Schmitt, H. W. (1972). "Prompt gamma-rays emitted in the thermal-neutron-induced fission of uranium-235 " Physical Review C: Nuclear Physics **6**(3): 1023-1039.

Rhodes, R. (1986). The Making of the Atomic Bomb, Simon and Schuster.

Schuler, R. H., Allen, A. O. (1957). "Radiation chemistry studies with cyclotron beams of variable energy-yields in aerated ferrous sulfate solution " J Am Chem Soc **79**: 1565-1572.

Schuler, R. H., Barr, N. F. (1956). "Oxidation of ferrous sulfate by ionizing radiations from (n,a) reactions of boron and lithium." J Am Chem Soc **78**: 5756–5762.

Schulz, W. W., Burger, L. L., Navratil, J. D., Bender, K. P. (1984). Science and Technology of Tributyl Phosphate Volume III Applications of Tributyl Phosphate in Nuclear Fuel Processing. Boca Raton, Florida, CRC Press, Inc.

Schulz, W. W., Navratil, J. D., Talbot, A. E. (1984). Science and Technology of Tributyl Phosphate, Volume I: Synthesis, Properties, Reaction and Analysis, Chapter 7 Radiolytic Behavior p. 221-263. Boca Raton, FL, CRC Press.

Science, U. S. D. o. E. O. o. (1998). Research Needs and Opportunities In Radiation Chemistry.

Stieglitz, L., Becker, R. (1983). "Chemical and radiolytic solvent degradation in the PUREX process." Nukleare Entsorgung (Saf. Nucl. Fuel Cycle): 333-350.

Stieglitz, L., Becker, R. (1984). Chemical and radiolytic degradation in the Purex process. Fuel Reprocessing and Waste Management, Am. Nucl. Soc. Int. Top. Meet. **1:** 451-458.

Stollenwerk, A. H., Weishaupt, M., Stieglitz, L., Becker, R. (1989). "Is solvent radiolysis a safety problem for PUREX plant performance?" Nukleare Entsorgung (Saf. Nucl. Fuel Cycle) **4**: 85-106.

Sugo, Y., Taguchi, M., Sasaki, Y., Hirota, K., Kimura, T. (2009). "Radiolysis study of actinide complexing agent by irradiation with helium ion beam." Radiat. Phys. Chem. **78**(12): 1140-1144.

Tripathi, S. C., Sumathi, S., Ramanujam, A. (1999). "Effects of Solvent Recycling on Radiolytic Degradation of 30% Tributyl Phosphate–n-Dodecane–HNO3 System." Separation Science and Technology **34**(14): 2887–2903.

Vladimirova, M. V., Kulikov, I. A. (1986). "Kinetics of tributyl phosphate radiolytic decomposition." Atomnaya Energiya **60**(3): 195-197.

Vladimirova, M. V., Kulikov, I. A., Bulkin, V. I., Sosnovskii, O. A. (1987). "Kinetics of radiolytic processes in tributyl phosphate." Atomnaya Energiya **62**(4): 273–274.

Vladimirova, M. V., Kulikov, I. A., Bulkin, V. I., Sosnovskii, O. A. (1989). "Kinetics of radiolytic decomposition of tributyl phosphate in mono- and two-phase systems." Radiokhimiya **31**(1): 36-39.

Weaver, B., Kappelmann, F. A., (1964). Talspeak: a new method of separating americium and curium from the lanthanides by extraction from an aqueous solution of an aminopolyacetic acid complex with a monacidic organophosphate or phosphonate, U.S. At. Energy Comm., ORNL-3559.

Wilkinson, R. W., Williams, T. F. (1961). "The radiolysis of tri-n-alkyl phosphates." J. Chem. Soc.: Paper 801, 4098-4107.

Williams, T. F., Wilkinson, R. W. (1957). The Radiolysis of tri-n-butyl phosphate and allied systems. A.E.R.E. Report C/R 2179.